

AN X-RAY DIFFRACTION INVESTIGATION  
OF SILVER AZIDE AND BORIC OXIDE  
AND AN ELECTRON DIFFRACTION INVESTIGATION OF  
SOME THREE-MEMBERED RINGS AND SOME HALOGENATED METHANES

Thesis by

Heinz Gerhard Pfeiffer

In Partial Fulfillment of the Requirements  
For the Degree of  
Doctor of Philosophy

California Institute of Technology  
Pasadena, California

1948

## ACKNOWLEDGEMENTS

I wish to express my sincere appreciation to Dr. E. W. Hughes and Dr. V. Schomaker for the great amount of help and encouragement extended during the course of these investigations, and to Dr. Linus Pauling for his continuing interest and the many valuable suggestions he has made.

My associates, Mr. A. M. Soldate, Dr. D. P. Shoemaker, Mr. B. Keilin, and Mr. G. Guthrie, have assisted me greatly during the entire course of my graduate work, and I wish to express my appreciation to them at this time.

I am indebted to my wife, Alma, for her painstaking help in the preparation of this thesis.

## ABSTRACT

Sections I and II report the X-ray diffraction investigations of silver azide and boric oxide. Silver azide crystallizes in a body-centered orthorhombic structure. The space group is  $Ibam$  with four molecules in the unit cell. The silver atoms are in (a), the central nitrogens in (d), and the end nitrogens in (j) with  $\underline{x} = 0.156$  and  $\underline{y} = 0.369$ . A new type of part cell projection is developed. Boric oxide crystallizes in a hexagonal structure with three molecules in the unit cell,  $\underline{a}_0 = 4.320$  Kx.,  $\underline{c}_0 = 8.139$  Kx. Each boron has three bonded oxygen neighbors at a distance of  $1.35 \text{ \AA}$  and coplanar with the boron.

Sections III and IV report electron diffraction investigations of some three-membered rings and some halogenated methanes. The HCH bond angles of cyclopropane are about  $116^\circ$ , the C-H distance  $1.10$  Kx., and the C-C distance  $1.515$  Kx. The other three-membered rings...ethylene imine, ethylene oxide, ethylene sulfide, and N-methyl ethylene imine...have HCH angles of  $116^\circ$  and all other distances close to the sum of the covalent radii. The halogenated methanes...difluorobromomethane, trifluorobromomethane, trichlorobromomethane, and difluorodibromomethane...have bond angles close to tetrahedral; the only significant deviation is the FCB $\alpha$  angle of  $110.5^\circ$  in trifluorobromomethane. The bond lengths in these compounds are close to the sum of the covalent radii with the exception of the C-Br in difluorodibromomethane ( $1.925$  Kx.) and in trifluorobromomethane ( $1.89$  Kx.).

## TABLE OF CONTENTS

	<u>Page No.</u>
Part A - X-Ray Diffraction	
I. Silver Azide . . . . .	1
II. Boric Oxide . . . . .	18
Part B - Electron Diffraction	
III. The Three-Membered Rings . . . . .	33
Cyclopropane . . . . .	34
Ethylene Imine . . . . .	42
Ethylene Oxide . . . . .	46
N-Methyl Ethylene Imine . . . . .	50
Ethylene Sulfide . . . . .	52
IV. The Halogenated Methanes . . . . .	57
Difluorobromomethane . . . . .	58
Trifluorobromomethane . . . . .	62
Trichlorobromomethane . . . . .	65
Difluorodibromomethane . . . . .	67
Bibliography . . . . .	75

PART A

THE X-RAY DIFFRACTION INVESTIGATION  
OF  
SILVER AZIDE AND BORIC OXIDE

# I. An X-Ray Diffraction Study of the Structure of Silver Azide, $\text{AgN}_3$

The structure of the heavy metal azides is of considerable interest on account of the ease with which they detonate. Ionic azides such as sodium azide,  $\text{NaN}_3$ , potassium azide,  $\text{KN}_3$ , and ammonium azide,  $\text{NH}_4\text{N}_3$ , can be heated to decomposition without exploding. Such covalent azides as methyl azide,  $\text{CH}_3\text{N}_3$ , cyanuric triazide,  $\text{C}_3\text{N}_3(\text{N}_3)_3$ , and hydrazoic acid,  $\text{HN}_3$ , detonate readily. It was felt that there was a possibility that the explosive character of silver azide could be explained on the basis of its structure.

The ionic azides (1) have a symmetrical linear azide ion with bonded N-N distances of about 1.15 Å. The covalently bound azide groups (2) are asymmetrical and linear with bonded N-N distances of about 1.12 Å and 1.24 Å. No complete investigation of a heavy metal azide has yet been made. Bassiere (3), West (4), and Hughes (5) have investigated silver azide, and Wilsdorf (6) has investigated cuprous azide,  $\text{CuN}_3$ . The results of the investigations of silver azide are given in Table I.

The three results for silver azide agree as to space group and the positions of the silver and  $\text{N}_I$ (central). The agreement of the axial lengths is fair, but West's density is certainly low. The parameters reported by Bassiere are certainly in error for they would demand that  $F(\underline{hkl}) = F(\underline{khl})$ , while a glance at the observed values (Table II), particularly

Table I

	<u>a<sub>0</sub></u>	<u>b<sub>0</sub></u>	<u>c<sub>0</sub></u>	<u>ρ obs.</u>	<u>ρ calc.</u>
Bassiere	5.58 Kx.	5.93 Kx.	6.04 Kx.	4.81 g/cc	4.99 g/cc
West	5.58 Kx.	5.90 Kx.	5.96 Kx.	4.50 g/cc	5.06 g/cc
Hughes	5.59 Kx.	5.88 Kx.	6.00 Kx.	4.837 g/cc	5.04 g/cc

	<u>Ag</u>	<u>N<sub>I</sub>(central)</u>	<u>N<sub>II</sub>(end)</u>	<u>Z</u>	<u>Space Group</u>
Bassiere	( <u>a</u> )	( <u>d</u> )	( <u>j</u> ) $\frac{x}{y} = \frac{0.145}{0.145}$	4	Ibam-D <sub>2h</sub> <sup>26</sup>
West	( <u>a</u> )	( <u>d</u> )	( <u>j</u> ) $\frac{x}{y} = \frac{0.155}{0.375}$	4	Ibam-D <sub>2h</sub> <sup>26</sup>
Hughes	( <u>a</u> )	( <u>d</u> )	not determined	4	Ibam-D <sub>2h</sub> <sup>26</sup>

The origin used by Bassiere and by West and the axes used by West have been changed to conform with those used in this thesis; the origin and special positions are as given in "Internationale Tabellen zur Bestimmung von Kristallstrukturen."

those with  $l$  odd, shows that these intensities are quite different. Both West and Wilsdorf assumed the configuration and dimensions of the azide group to be the same as in the ionic azides; an assumption which does not seem, a priori, very sound. West used only six reflections from the odd layer lines which are caused by the  $N_{II}(\text{end})$  alone. Wilsdorf's determination was made with only powder data. It therefore seemed desirable to do a complete investigation of silver azide and determine the parameters directly from the intensity data.

The crystals used in this investigation were made by adding silver azide to aqueous ammonia solution containing just enough ammonia to dissolve the silver azide. The crystals grown in a few days by cooling or evaporating the solutions gave evidence of twinning, a difficulty also mentioned by Bassiere (3), the faces were striated and the observed X-ray reflections were often doubled. Finally some of the solution was put away for two years in a cork-stoppered test tube, and at the end of this time the solution had evaporated and left needle-like crystals of silver azide that showed no evidence of twinning.

Pyroelectric experiments were negative. Goniometric measurements on the well developed  $110$  faces gave  $a_0 : b_0 = 0.946$ . The Laue symmetry is  $mmm$ . An average of the values of West, Bassiere, and Hughes was taken for the axial lengths,

i.e.,  $a_0 = 5.58$  Kx.,  $b_0 = 5.90$  Kx., and  $c_0 = 6.00$  Kx. From these  $a_0 : b_0 = 0.946$ , in agreement with the goniometric value.

A complete set of  $20^\circ$  oscillation photographs was made about the  $c_0$  axis using Mo  $K\alpha$  radiation. Five layer lines were observed on each side of the equator. A rotation photograph about the  $c_0$  axis was also made to facilitate comparison of the intensities of the  $hkl$  and  $khl$  reflections. Multiple film technique was used with 0.001" Cu foil between films. The film factor, 4, was calculated from the film factor of Eastman No Screen film for Cu  $K\alpha$  radiation, 3.7, and the absorption coefficient for Cu. It is estimated from comparison of four independent sets of intensity estimations that the  $hk0$  reflection intensities are accurate to 20%, and the  $hkl$  reflection intensities are slightly more accurate. Two films were used in the oscillation photographs and three in the rotation photographs. All intensities were estimated visually (Table II) and all  $hkl$  and  $khl$  reflections were compared individually, special care being taken with the odd layer lines which depend, as shown below, only on the  $N_{II}$  parameters. The observed intensities were corrected with Lorentz and polarization and Cox-Shaw factors, and for absorption.

All reflections are absent for which  $h+k+l$  is odd and  $h0l$  and  $0kl$  are absent with  $l$  odd. Exceptions to these

latter rules were carefully sought since the reflections with  $\underline{l}$  odd are all weak; even with long exposures and favorable correction factors no exceptions were found. Possible space groups are Iba and Ibam. The negative result of the pyroelectric experiment indicates Ibam is more probable. It was observed that the 0th and 4th, and the 1st and 3rd layer lines showed the same dependence of the structure factors on  $\underline{h}$  and  $\underline{k}$ . The structure factors for these space groups are:

Ibam

$$\begin{array}{l} \underline{h} + \underline{k} + \underline{l} \text{ even} \\ \left( \begin{array}{l} \underline{l} \text{ even} \\ \underline{l} \text{ odd} \end{array} \right. \end{array} \begin{array}{l} A = 16 \cos 2\pi \underline{hx} \cos 2\pi \underline{ky} \cos 2\pi \underline{lz} \\ B = 0 \\ A = -16 \sin 2\pi \underline{hx} \sin 2\pi \underline{ky} \cos 2\pi \underline{lz} \\ B = 0 \end{array}$$

Iba

$$\begin{array}{l} \underline{h} + \underline{k} + \underline{l} \text{ even} \\ \left( \begin{array}{l} \underline{l} \text{ even} \\ \underline{l} \text{ odd} \end{array} \right. \end{array} \begin{array}{l} A = 8 \cos 2\pi \underline{hx} \cos 2\pi \underline{ky} \cos 2\pi \underline{lz} \\ B = 8 \cos 2\pi \underline{hx} \cos 2\pi \underline{ky} \sin 2\pi \underline{lz} \\ A = -8 \sin 2\pi \underline{hx} \sin 2\pi \underline{ky} \cos 2\pi \underline{lz} \\ B = -8 \sin 2\pi \underline{hx} \sin 2\pi \underline{ky} \sin 2\pi \underline{lz} \end{array}$$

It can be seen from the above structure factors that this functional dependence on  $\underline{h}$  and  $\underline{k}$  alone of alternate even and all odd layer lines will hold only if all of the  $\underline{z}$  parameters are 0, 1/4, 1/2 and 3/4. This permits only certain special positions in Ibam. If these values for  $\underline{z}$  are substituted in positions of Iba the resulting structure has Ibam symmetry. Ibam is therefore the most probable space group.

Placing the silver atoms in (a) sets the signs of all of the  $F(\underline{hkl})$  with  $\underline{l} = 2n$  since

$$4f_{Ag} > 12f_N$$

It was therefore possible to calculate a two-dimensional Fourier projection on the 001 plane (Fig. 1).

$$\rho(\underline{x}, \underline{y}) = \frac{1}{A} \sum_{\underline{h}} \sum_{\underline{k}} F(\underline{hk}0) \cos 2\pi (\underline{hx} + \underline{ky})$$

The  $N_{II}$ 's are at  $\underline{x} = 0, \underline{y} = \frac{1}{2}$  and  $\underline{x} = \frac{1}{2}, \underline{y} = 0$ , with two at each position. From a projection along the [110] axis made by Dr. Hughes using Cu  $K\alpha$  data the  $\underline{z}$  parameters of the nitrogens must be 0 and  $\frac{1}{2}$ ; they must therefore be in (d). The  $N_{II}$ 's are in (j) with  $\underline{x} = 0.153$  and  $\underline{y} = 0.389$ . From these approximate parameters the signs of the reflections on the odd layer lines were calculated.

A half cell projection  $\rho(\underline{x}, \underline{y}, -\frac{1}{4} \rightarrow \frac{1}{4})$  was made (7 & 8)

$$\begin{aligned} \rho(\underline{x}, \underline{y}, -\frac{1}{4} \rightarrow \frac{1}{4}) &= \frac{1}{2A} \sum_{\underline{h}} \sum_{\underline{k}} F(\underline{hk}0) \cos 2\pi (\underline{hx} + \underline{ky}) \\ &+ \frac{1}{\pi A} \sum_{\underline{h}} \sum_{\underline{k}} \sum_{\underline{l} \text{ odd}} \frac{F(\underline{hkl})}{\underline{l}} \cos 2\pi (\underline{hx} + \underline{ky}) \end{aligned}$$

This projection (Fig. 2) gave the parameters  $\underline{x} = 0.156$  and  $\underline{y} = 0.373$  but because the nitrogen contribution to the  $F(\underline{hk}0)$  was so small compared to the silver contribution it was decided to make a projection using only odd layer line data, which depends on the  $N_{II}$  alone. The Fourier projection  $\rho'(\underline{x}, \underline{y})$  (Fig. 3) shows only the  $N_{II}$  atoms.

The projection calculated (9) was

Only every tenth contour is shown for the silver atoms.

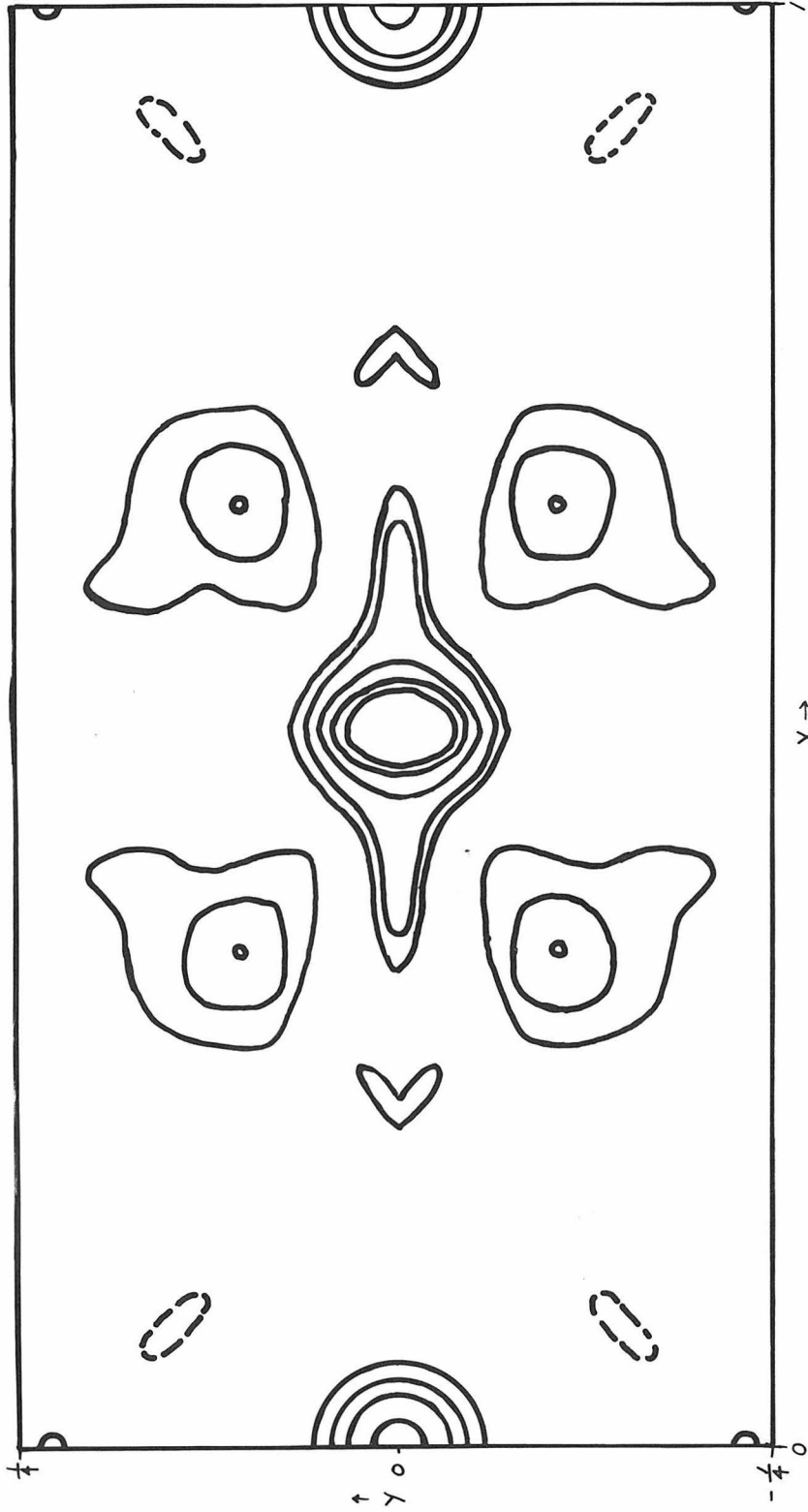
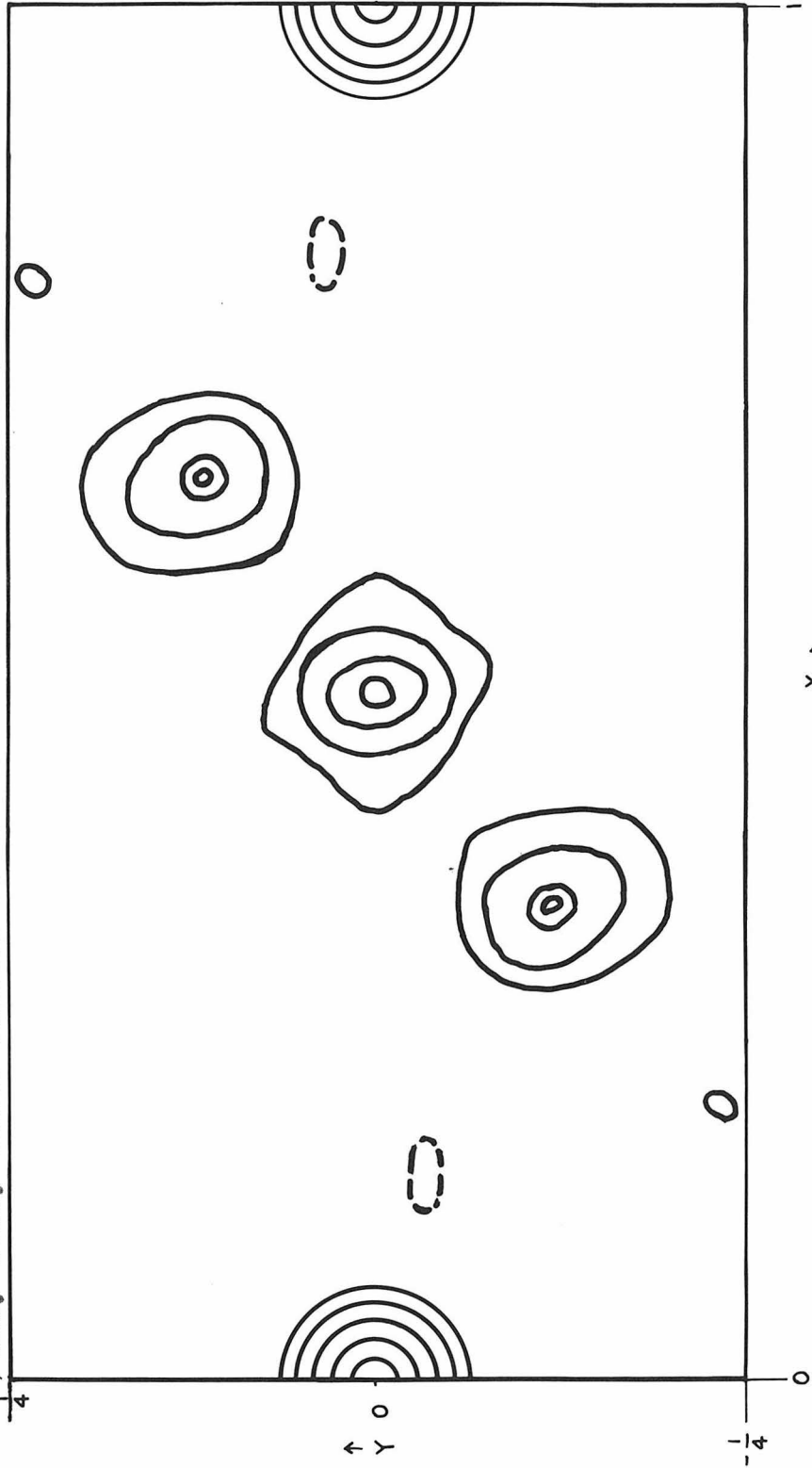


Figure 1  
Projection Along [001]

Only every tenth contour is shown for the silver atoms.



X →

Figure 2

Half-cell Projection Along [001]

$$\rho'(\underline{x}, \underline{y}) = \frac{2}{\pi A} \sum_{\underline{h}} \sum_{\underline{k}} \sum_{\substack{\underline{l} \\ \text{odd}}} \frac{F(\underline{hkl})}{\underline{l}} \cos 2\pi (\underline{hx} + \underline{ky}) \sin \frac{2\pi \underline{l}}{4}$$

If 
$$\rho'(\underline{x}, \underline{y}) = \int_{-\frac{1}{4}\underline{c}_0}^{\frac{1}{4}\underline{c}_0} \rho(\underline{x}, \underline{y}, \underline{z}) d\underline{z} - \int_{\frac{1}{4}\underline{c}_0}^{\frac{3}{4}\underline{c}_0} \rho(\underline{x}, \underline{y}, \underline{z}) d\underline{z}$$

$$\rho(\underline{x}, \underline{y}, \underline{z}) = \frac{1}{V} \sum_{\underline{h}} \sum_{\underline{k}} \sum_{\underline{l}} F(\underline{hkl}) \cos 2\pi \left( \frac{\underline{hx}'}{\underline{a}_0} + \frac{\underline{ky}'}{\underline{b}_0} \right) \cos 2\pi \frac{\underline{lz}'}{\underline{c}_0}$$

$$- F(\underline{hkl}) \sin 2\pi \left( \frac{\underline{hx}'}{\underline{a}_0} + \frac{\underline{ky}'}{\underline{b}_0} \right) \sin 2\pi \frac{\underline{lz}'}{\underline{c}_0} \quad \begin{array}{l} \underline{x}' = \underline{a}_0 \underline{x} \\ \underline{y}' = \underline{b}_0 \underline{y} \\ \underline{z}' = \underline{c}_0 \underline{z} \end{array}$$

The integral of  $\sin 2\pi \frac{\underline{lz}'}{\underline{c}_0}$  from  $-\frac{\underline{c}_0}{4} \rightarrow \frac{\underline{c}_0}{4}$  is zero,

and from  $\frac{\underline{c}_0}{4} \rightarrow \frac{3\underline{c}_0}{4}$  is zero.

The integral of  $\cos 2\pi \frac{\underline{lz}'}{\underline{c}_0}$  over this range is zero if  $\underline{l}$  is even.

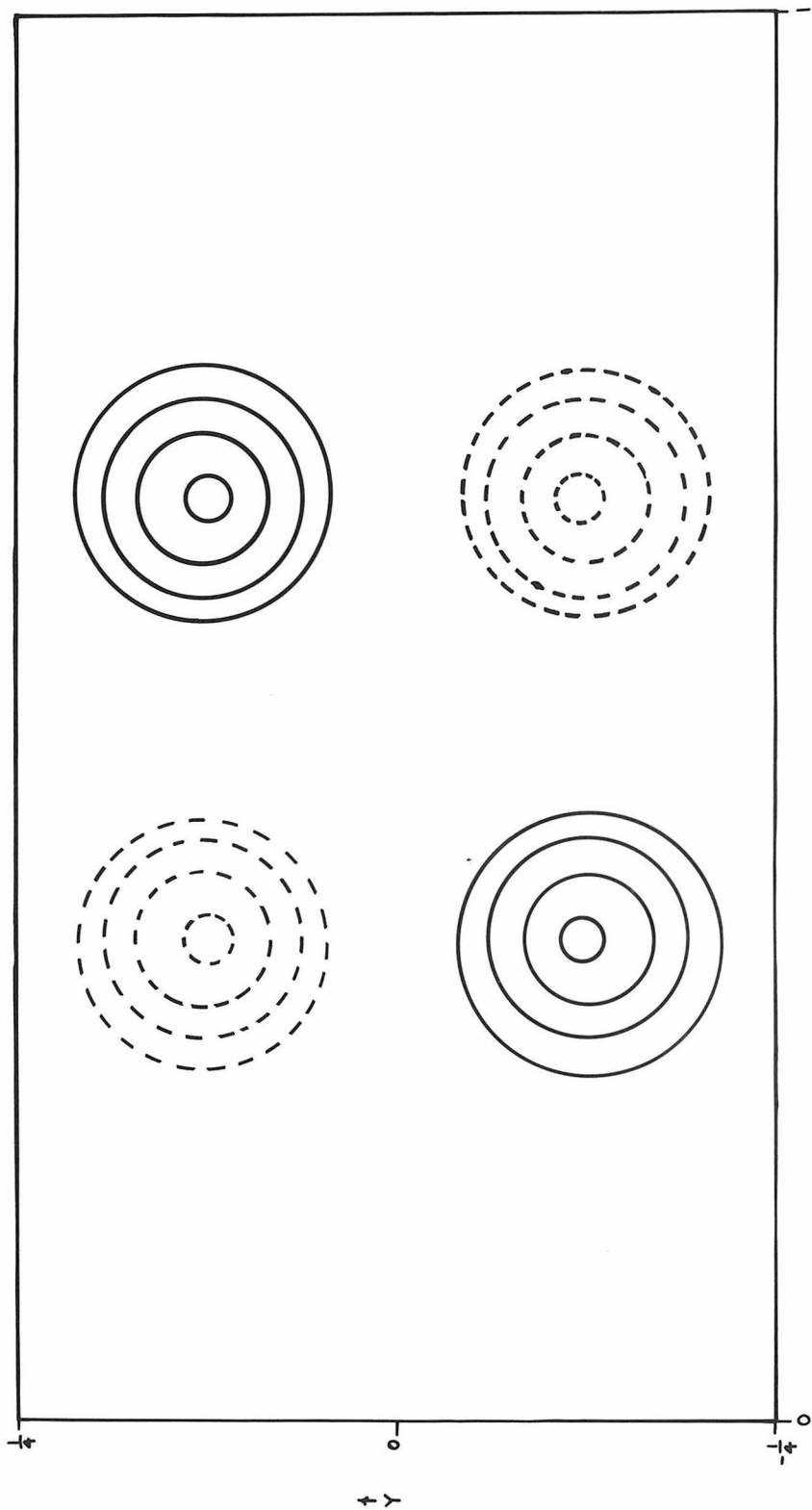
Therefore

$$\rho'(\underline{x}, \underline{y}) = \frac{1}{V} \sum_{\underline{h}} \sum_{\underline{k}} \sum_{\substack{\underline{l} \\ \text{odd}}} F(\underline{hkl}) \cos 2\pi \left( \frac{\underline{hx}'}{\underline{a}_0} + \frac{\underline{ky}'}{\underline{b}_0} \right)$$

$$\left\{ \int_{-\frac{\underline{c}_0}{4}}^{\frac{\underline{c}_0}{4}} \cos \frac{2\pi \underline{lz}'}{\underline{c}_0} d\underline{z}' - \int_{\frac{\underline{c}_0}{4}}^{\frac{3\underline{c}_0}{4}} \cos \frac{2\pi \underline{lz}'}{\underline{c}_0} d\underline{z}' \right\}$$

$$\rho'(\underline{x}, \underline{y}) = \frac{2}{\pi A} \sum_{\underline{h}} \sum_{\underline{k}} \sum_{\substack{\underline{l} \\ \text{odd}}} \frac{F(\underline{hkl})}{\underline{l}}$$

$$\cos 2\pi \left( \frac{\underline{hx}'}{\underline{a}_0} + \frac{\underline{ky}'}{\underline{b}_0} \right) \sin \frac{2\pi \underline{l}}{4}$$



x →

Figure 3

$$\rho(x, y)$$

This is the projection shown in Fig. 3. Atoms from  $z = 1/4$  to  $3/4$  are subtracted from those that lie from  $z = -1/4$  to  $1/4$ . This eliminates the silver atoms and central nitrogen atoms, leaving only those nitrogens,  $N_{II}$ , which have parameters. We are, in effect, taking the difference between the two half-cell projections along  $c_0$ . Four  $N_{II}$ 's are at  $z = 0$  and four at  $z = \frac{1}{2}$ , the first four show up positive and the second four negative. The final parameters from this projection are  $x = 0.156 \pm 0.002$ ,  $y = 0.369 \pm 0.002$ .

Table II shows the agreement of the calculated and observed structure factors. The  $F(hk0)$  data is first, arranged in order of decreased spacing, then the  $F(hkl)$  data with  $l$  odd, also arranged in order of decreasing spacing. A temperature factor,  $e^{-B\left(\frac{\sin \theta}{\lambda}\right)^2}$ , with  $B = 1$  was applied to the calculated  $F_0$ 's. The  $F$ 's observed were put on an absolute scale by averaging the ratios of  $F$  observed to  $F$  calculated. Scattering factors for silver and nitrogen were taken from the "Internationale Tabellen zur Bestimmung von Kristallstrukturen."

Table III shows the nearest neighbor distance, and a drawing of the structure is shown in Figure 4. This is a projection along  $c_0$  onto (001).

The large heavy circles are nitrogens at  $z = 0$ , the large light circles nitrogens at  $z = \frac{1}{2}$ , and the small medium circles are silver at  $z = \frac{1}{4}$ , the silvers at  $3/4$  lie directly

Table II

<u>h</u>	<u>k</u>	<u>0</u>	<u>F</u> <u>calc.</u>	<u>F</u> <u>obs.</u>	<u>h</u>	<u>k</u>	<u>0</u>	<u>F</u> <u>calc.</u>	<u>F</u> <u>obs.</u>
1	1	0	127	121	7	7	0	29	28
0	2	0	167	135	2	10	0	31	25
2	0	0	152	135	6	8	0	39	37
2	2	0	148	139	8	6	0	35	36
1	3	0	117	129	5	9	0	26	23
3	1	0	127	140	10	0	0	27	29
0	4	0	98	105	10	2	0	28	20
4	0	0	99	121	9	5	0	23	19
3	3	0	78	88	4	10	0	24	17
2	4	0	113	109	1	11	0	22	17
4	2	0	104	107	10	4	0	24	17
1	5	0	86	91					
5	1	0	80	92					
4	4	0	92	108					
3	5	0	61	61					
0	6	0	84	75					
5	3	0	73	73					
6	0	0	88	93					
2	6	0	73	64					
6	2	0	71	65					
1	7	0	53	52					
5	5	0	57	64					
4	6	0	64	64					
7	1	0	46	56					
6	4	0	53	53					
3	7	0	57	60					
0	8	0	63	61					
7	3	0	53	55					
2	8	0	50	47					
8	0	0	51	52					
8	2	0	47	51					
6	6	0	47	42					
5	7	0	39	42					
7	5	0	34	36					
1	9	0	36	33					
4	8	0	40	37					
8	4	0	42	37					
3	9	0	31	23					
9	1	0	35	35					
0	10	0	36	30					
9	3	0	29	25					

Per cent deviation 9.8				
<u>h</u>	<u>k</u>	<u>l</u>	<u>F</u> <u>calc.</u>	<u>F</u> <u>obs.</u>
1	2	1	29	27
2	1	1	-22	24
1	2	3	19	19
2	1	3	-14	13
2	3	1	-13	13
3	2	1	3	3
1	4	1	-1	<3
4	1	1	9	8
2	3	3	-11	10
3	2	3	2	<3
1	4	3	-1	<3
3	4	1	-1	<3
4	3	1	7	7
2	5	1	9	9
3	4	3	-1	<3
4	3	3	4	3
5	2	1	-12	13
4	1	3	6	5
2	5	3	8	6
5	2	3	-10	8
1	6	1	-8	7
6	1	1	3	3

Per cent deviation 8.2			
------------------------	--	--	--

under the silvers at 1/4. All bonds go in the direction of their taper.

Table III

<u>Atom</u>	<u>Number</u>	<u>Neighbor</u>	<u>Distance</u>
Ag	4	N <sub>II</sub>	2.56 Å
	4	N <sub>II</sub>	2.79 Å
	4	N <sub>I</sub>	3.16 Å
	4	N <sub>I</sub>	3.31 Å
	2	Ag	3.00 Å
N <sub>I</sub>	2	N <sub>II</sub>	1.16 Å
	2	N <sub>I</sub>	3.00 Å
N <sub>II</sub>	2	N <sub>II</sub>	3.13 Å
	2	N <sub>II</sub>	3.12 Å
	2	N <sub>II</sub>	3.38 Å
	2	N <sub>II</sub>	3.47 Å

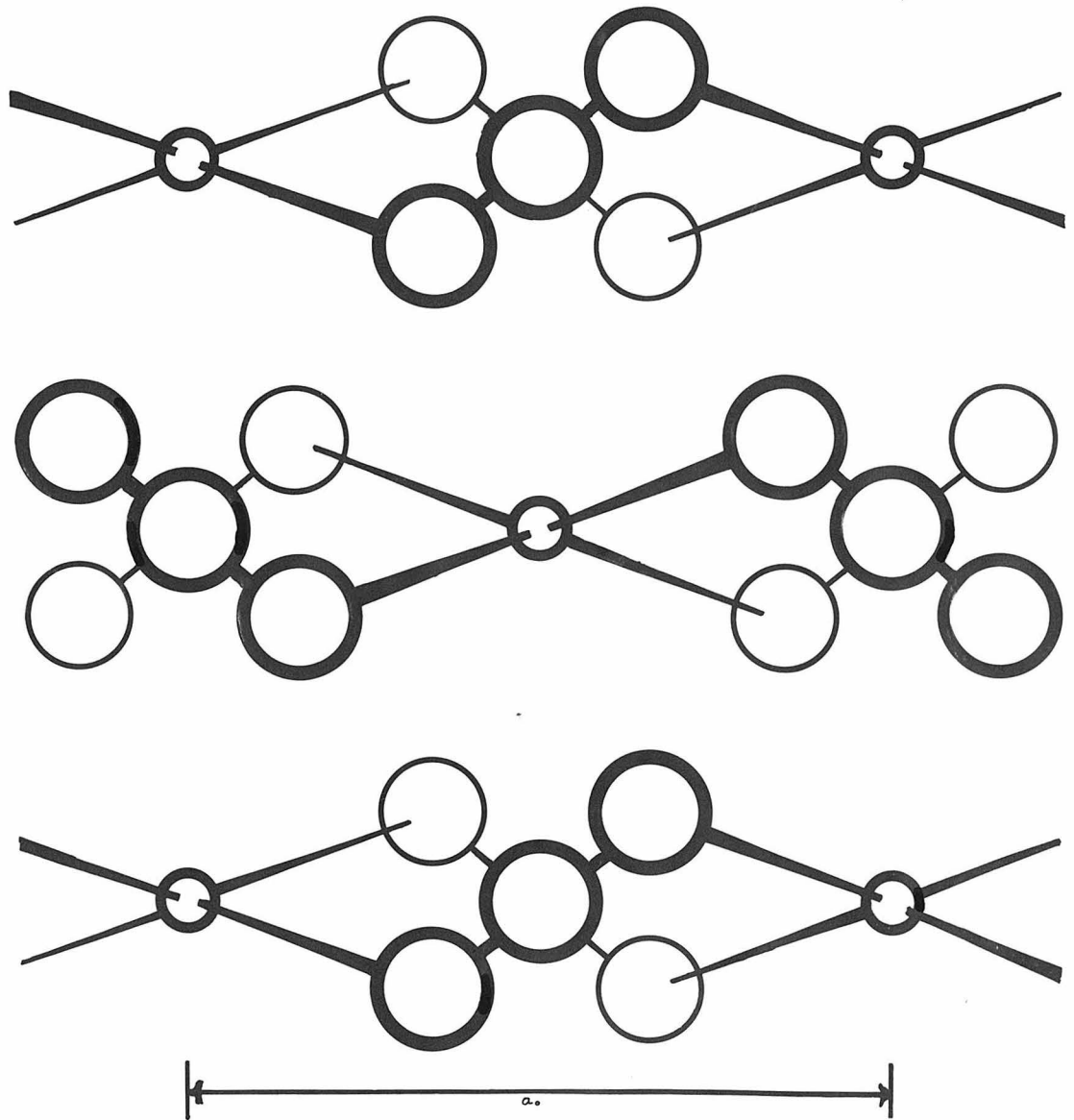


Figure 4

Projection of the Structure of  
Silver Azide on the x-y Plane

DISCUSSION. The structure is a distorted potassium azide structure. In potassium azide, which is tetragonal, each potassium ion is surrounded by eight  $N_{II}$ 's at the corners of a square Archimedes antiprism. In silver azide in order to satisfy the silver coordination of four, four of the nitrogens are repelled and four drawn closer in orthorhombic symmetry. The four that are drawn closer are at the ends of opposite side diagonals of the antiprism. This has the effect of distorting the square base into a rhombus with the short diagonal in the direction of bonding.

Ammonium azide is also a distorted potassium azide structure (10). If in potassium azide the azide groups are arranged so as to give cubic symmetry, i.e., each layer is identical with the one below, and then four  $N_{II}$ 's are pulled closer and four pushed away, there will also be fourfold coordination that is now almost precisely tetrahedral. That is the  $NH_4N_3$  structure. The  $NH_4^+$  has a strong tendency to form four tetrahedral hydrogen bonds and can satisfy this desire in this way. The larger size of the ammonium ion would make a silver azide structure improbable for ammonium azide because the  $NH_4^+$  would be brought too close together.

The azide group in silver azide has a center of symmetry and is linear with a bonded distance of  $1.16 \pm 0.02 \text{ \AA}$ . Each azide is bonded to four silvers, two being attached to each end. The bond angles around the silver are

about  $85^\circ$ ,  $85^\circ$ ,  $108^\circ$  and  $108^\circ$ . The bonding runs in the x and z directions making this a layer structure.

The silver nitrogen bonded distance is  $2.56 \text{ \AA}$ , considerably lengthened over the sum of the single bond covalent radii,  $2.23 \text{ \AA}$ , but much less than the van der Waal's distance which is  $2.8 \text{ \AA}$ . If each bond is only a fourth of a covalent bond, the expected lengthening can be calculated from Pauling's relation (11)

$$\Delta r = 0.300 \log n \quad n = \text{bond number}$$

$$\Delta r = 0.18 \text{ \AA}$$

From this calculation the expected silver-nitrogen distance would then be  $2.59 \text{ \AA}$  in good agreement with the value found.

The silver-silver distance  $3.00 \text{ \AA}$  is also of interest. The sum of the covalent single bond radii of silver is  $3.06 \text{ \AA}$ , the sum of the metallic radii for tetrahedral coordination is  $2.70 \text{ \AA}$ . It seems that the silver-silver distance is less than would be predicted considering the silvers to be covalent and not bonded to each other.

$\text{CuN}_3$  (12) can also be derived from the potassium azide structure, a fact not recognized by Wilsdorf. If one orients the  $\text{N}_3$  groups lying on the  $[021]$  axes of  $\text{KN}_3$  parallel to each other and the ones on the  $[201]$  axes parallel to each other but at right angles to the first series the structure

will be close to the  $\text{CuN}_3$  structure.

From the results of this investigation there is no obvious explanation of the explosive properties of silver azide.

RESULTS. Silver azide crystallizes in a body-centered orthorhombic structure with space group,  $\text{Ibam-D}_{2h}^{26}$ , and with  $\underline{a}_0 = 5.58 \pm 0.02$  Kx.,  $\underline{b}_0 = 5.90 \pm 0.02$  Kx. and  $\underline{c}_0 = 6.00 \pm 0.02$  Kx. There are four molecules in the unit cell with the silver in (a), the  $\text{N}_I$  (central) in (d) and the  $\text{N}_{II}$  (end) in (j) with  $\underline{x} = 0.156 \pm 0.002$  and  $\underline{y} = 0.369 \pm 0.002$ . The bonded nitrogen-nitrogen distance is  $1.16 \pm 0.02$  Å and the bonded silver-nitrogen distance is  $2.56 \pm 0.02$  Å. Punched cards were used for all Fourier calculations (13).

## II. An X-Ray Diffraction Study of Boric Oxide

The preparation of crystalline boric oxide,  $B_2O_3$ , has been reported by Taylor and Cole (14), McCulloch (15), and Kracek, Morey and Merwin (16). Taylor and Cole reported a crystalline phase, which they report as  $B_2O_3$ , formed upon holding  $HBO_2$  in a vacuum at  $200^\circ C$  for several days and 400 hours more at  $225^\circ C$ . The density was 1.805 g/cc and the melting point  $294 \pm 1^\circ C$ . This density is less than that of  $B_2O_3$  glass, 1.844 g/cc. Morey and Merwin (17) attempted to repeat this experiment, with no success. McCulloch reports the formation of crystalline  $B_2O_3$  after heating  $H_3BO_3$  in loosely covered metal cans for several days at  $300^\circ C$ . The density he reports is 2.42 g/cc and the melting point  $460^\circ - 470^\circ C$ . The results of Kracek, Morey, and Merwin are in agreement with those of McCulloch. The crystalline  $B_2O_3$  prepared by McCulloch showed 37 powder lines using  $CuK\alpha$  radiation.

The sample of crystalline  $B_2O_3$  used in this investigation was procured by Dr. Max T. Rogers. Dr. Rogers and Dr. Hughes took a series of multiple film powder photographs using 3 films with both  $CuK\alpha$  and  $FeK\alpha$  radiation. Forty-four lines were observed after subtracting known lines due to traces of  $HBO_2$  and  $H_3BO_3$ .

The lines were indexed by Dr. Hughes using an adaptation of the method of Jacob and Warren (18). Table IV shows the agreement between observed and calculated values of  $\frac{1}{d^2}$

Table IV

<u>h</u> <u>k</u> <u>l</u>	$\frac{1}{\underline{d}^2}$ calc.	$\frac{1}{\underline{d}^2}$ obs.	<u>h</u> <u>k</u> <u>l</u>	$\frac{1}{\underline{d}^2}$ calc.	$\frac{1}{\underline{d}^2}$ obs.
1 0 0	.0714	.0719	3 0 4	.8740	.8720
1 0 1	.0859	.0856	2 2 2	.9149	.9140
1 0 2	.1292}	.1287	1 1 7	.9224}	.9293
0 0 3	.1301}		1 3 0	.9286}	
1 0 3	.2015	.2013	1 3 1	.9431	.9420
1 1 0	.2143	.2149	1 3 2	.9864}	.9870
1 1 1	.2288	.2280	2 2 3	.9872}	
1 1 2	.2721	.2715	2 0 7	.9938}	.9920
2 0 0	.2857	.2865	1 0 8	.9963}	
2 0 1	.3002}	.3007	1 2 6	1.0202	1.018
1 0 4	.3026}		1 3 3	1.0587	1.056
2 0 2	.3435}	.3433	1 1 8	1.1392}	1.139
1 1 3	.3444}		4 0 0	1.1428}	
2 0 3	.4158	.4158	4 0 1	1.1573}	1.1565
1 0 5	.4327	.4320	1 3 4	1.1598}	
1 1 4	.4455	--	3 0 6	1.1630}	1.1635
1 2 0	.5000	.5003	0 0 9	1.1705}	
1 2 1	.5145}	.5155	4 0 2	1.2006}	1.202
2 0 4	.5169}		1 2 7	1.2081}	
0 0 6	.5202}	.5580	2 0 8	1.2184}	--
1 2 2	.5578		1 0 9	1.2419	1.240
1 1 5	.5756	.5755	4 0 3	1.2729	1.261
1 0 6	.5916	.5920	1 3 5	1.2899	1.289
1 2 3	.6301	.6295	3 0 7	1.3509}	1.352
3 0 0	.6428}	.6446	2 3 0	1.3571}	
2 0 5	.6470}		2 3 1	1.3716}	
3 0 1	.6573	.6575	4 0 4	1.3740}	1.1375
3 0 2	.7006	.7000	2 2 6	1.3773}	
1 2 4	.7312}	.7315	2 3 2	1.4149	1.4135
1 1 6	.7345}		1 2 8	1.4245	
3 0 3	.7724}	{.7740}	1 3 6	1.4488}	1.446
1 0 7	.7795}	{.7765}	2 0 9	1.4562}	
2 0 6	.8059	.8065	2 3 3	1.4872	1.4835
2 2 0	.8571}	.8597	1 4 1	1.5145}	1.513
1 2 5	.8613}		1 0 10	1.5165}	
2 2 1	.8716	.8720			

A least squares calculation using 16 single lines gives

$\underline{a}_0 = 4.320 \text{ Kx.}$

$\underline{c}_0 = 8.319 \text{ Kx.}$

for the hexagonal unit cell with  $a_0 = 4.320$  Kx.,  $c_0 = 8.139$  Kx. and  $Z = 3$ . Several space groups are possible with the observed extinctions  $00\bar{l}$  with  $l = 1, 2, 5, \text{ and } 7$ . The presence or absence of  $00\bar{l}$  with  $l = 3, 4, 6, 8$  or  $9$  was unobservable on account of overlapping of lines.

The present part of the investigation started with attempts to grow single crystals by seeding vitreous  $B_2O_3$  at temperatures from  $200$  to  $450^\circ C$  and cooling slowly. Only microcrystals were obtained. Attempts were then made to grow crystals from a  $NaCl - AlCl_3$  melt but with no success. It was then decided to investigate the environment of each boron by means of a radial distribution sum

$$rD(\underline{r}) = \sum_{\underline{s}} |F_{\underline{s}}|^2 \frac{\sin \underline{s} \underline{r}}{\underline{s} \underline{r}}$$

In order to interpret the areas under the peaks in terms of numbers of nearest neighbors it was necessary to put the  $|F_0|^2$  on an absolute scale. The intensities (Table V) were estimated by integrating under the peaks on a microphotometer trace. The absolute scale and temperature factor were calculated by a method suggested in outline by Hettich (19) and developed independently by Shoemaker (20), Harker (21), and Hughes (22). The method suggested by Hughes was used; it differs from that of Harker in that it uses  $F$ 's rather than  $\hat{F} = \frac{F}{\sum_i f_i}$  and the equations

$$\log \frac{\sum_{\underline{s}} |F'|^2}{\sum_{\underline{s}} \sum_{\underline{i}} f_{\underline{i}}^2} = 2B\underline{s}^2 + 2 \log \underline{k}$$

are solved by least squares rather than graphically.

$$F(\underline{hkl}) = \sum_{\underline{i}} f_{\underline{i}} e^{2\pi \underline{i}\theta_{\underline{i}}} \quad \theta_{\underline{i}} = \underline{h}\underline{x}_{\underline{i}} + \underline{k}\underline{y}_{\underline{i}} + \underline{l}\underline{z}_{\underline{i}}$$

$$F(\underline{hkl}) \cdot F^*(\underline{hkl}) = |F|^2(\underline{hkl}) = \sum_{\underline{i}} f_{\underline{i}}^2 + \sum_{\underline{i} \neq \underline{j}} \sum_{\underline{j}} f_{\underline{i}} f_{\underline{j}} e^{2\pi \underline{i}(\theta_{\underline{i}} - \theta_{\underline{j}})}$$

If both sides are summed over the reciprocal lattice, for convenience over  $\underline{s}$  ( $\underline{s} = 4\pi \frac{\sin \theta}{\lambda}$ ), the last term will average out and

$$\sum_{\underline{s}} |F|^2(\underline{hkl}) = \sum_{\underline{s}} \sum_{\underline{i}} f_{\underline{i}}^2$$

where  $f_{\underline{i}} = f_{\underline{i}0} e^{-B\underline{s}^2}$ ,  $f_{\underline{i}0}$  being the atomic scattering

factor as reported in the "Internationale Tabellen zur Bestimmung von Kristallstrukturen," for stationary atoms.

The observed intensities, corrected for Lorentz and polarization,  $|F'|^2$ , are related to the absolute intensities,  $|F|^2$ , by the scale factor  $\underline{k}^2$ . Making these substitutions the equation becomes

$$k^2 \sum_{\underline{s}} |F'|^2 = \sum_{\underline{s}} \sum_{\underline{i}} f_{\underline{i}}^2 e^{-2B\underline{s}^2}$$

If the assumption is made that this equation holds over smaller intervals of  $\underline{s}$ , and it will if a representative number of  $|F'|^2$  are included in the interval in  $\underline{s}$ , then it is possible to derive a series of equations of the form

$$k^2 \sum_{\underline{s}=\underline{a}}^{\underline{b}} |F'|^2 = \sum_{\underline{s}=\underline{a}}^{\underline{b}} \sum_{\underline{i}} f_{\underline{i}}^2 e^{-2B\underline{s}^2}$$

Assuming that  $\underline{s}^2$  has its average value throughout the interval it is possible to take the logarithms of these equations

$$\log \frac{\sum_{\underline{s}=\underline{a}}^{\underline{b}} \sum_{\underline{i}} f_{\underline{i}}^2}{\sum_{\underline{s}=\underline{a}}^{\underline{b}} |F'|^2} = 2B\underline{s}_{\underline{a}\underline{b}}^2 + 2 \log k$$

$$\underline{s}_{\underline{a}\underline{b}}^2 = \overline{\underline{s}^2} \text{ from } \underline{a} \text{ to } \underline{b}$$

Such a series of equations derived from the  $B_2O_3$  data was solved by least squares methods; the temperature factor  $B$  obtained was 0.75, and the factor  $k$  was evaluated simultaneously. The intensities were then put on the absolute scale (Table V) with this factor and the radial distribution sum was calculated.

Table V

$\frac{\sin \theta}{\lambda}$	$h \ k \ l$	$\frac{p F ^2}{\text{obs.}}$	$\frac{\sin \theta}{\lambda}$	$h \ k \ l$	$\frac{p F ^2}{\text{obs.}}$
.060	0 0 1	0	.478	2 2 2	87
.121	0 0 2	0	.480	1 1 7)	
.1335	1 0 0	1.86	.481	0 0 8)	150
.1464	1 0 1	888	.481	1 3 0)	
.1795	1 0 2)		.485	1 3 1)	955
.1803	0 0 3)	3450	.496	1 3 2)	
.224	1 0 3	1390	.496	2 2 3)	867
.231	1 1 0	89	.498	2 0 7)	
.239	1 1 1	2470	.499	1 0 8)	
.240	0 0 4	0	.501	3 0 5	0
.261	1 1 2	566	.505	1 2 6	180
.267	2 0 0	267	.514	1 3 3	460
.274	2 0 1)		.522	2 2 4	0
.275	1 0 4)	648	.533	1 1 8)	478
.2925	2 0 2)		.534	4 0 0)	
.293	1 1 3)	1092	.537	4 0 1)	
.300	0 0 5	0	.538	1 3 4)	834
.322	2 0 3	397	.539	3 0 6)	
.329	1 0 5	670	.541	0 0 9)	
.333	1 1 4	0	.549	4 0 2)	
.354	1 2 0	356	.550	1 2 7)	312
.359	1 2 1)		.550	2 0 8)	
.359	2 0 4)	2025	.552	2 2 5	0
.361	0 0 6)		.557	1 0 9	177
.374	1 1 2	162	.564	4 0 3	71
.380	1 1 5	385	.568	1 3 5	202
.383	1 0 6	218	.581	3 0 7)	510
.397	1 2 3	300	.582	2 3 0)	
.401	3 0 0)		.585	2 3 1)	
.402	2 0 5)	430	.586	4 0 4)	364
.406	3 0 1	211	.587	2 2 6)	
.418	3 0 2	858	.588	1 1 9	0
.421	0 0 7	0	.595	2 3 2)	533
.427	1 2 4)		.597	1 2 8)	
.429	1 1 6)	1310	.600	0.0.10)	
.439	3 0 3)		.601	1 3 6)	143
.441	1 0 7)	810	.603	2 0 9)	
.448	2 0 6	113	.610	2 3 3	109
.462	2 2 0)		.613	1 4 0)	0
.464	1 2 5)	892	.614	4 0 5)	
.466	2 2 1)		.615	1 4 1)	405
.467	3 0 4)	58	.616	1.0.10)	

$$4\pi \underline{r} (\underline{r} D(\underline{r}) - \underline{r} |F_0|^2) = \frac{4\pi \underline{r}}{V} \sum_{\underline{s}} \frac{|F_{\underline{s}}|^2}{\underline{s}} \sin \underline{s} \underline{r}$$

$$|F_0|^2 = \frac{|F|^2 - \sum_{\underline{i}} f_{\underline{i}}^2}{(\sum_{\underline{i}} f_{\underline{i}})^2} e^{-\underline{a} \underline{s}^2}$$

The Patterson function (23) with provision for removing the peak at the origin and using a sharpening factor is given by

$$P(\underline{x}, \underline{y}, \underline{z}) = \frac{1}{V} \sum_{\underline{h}} \sum_{\underline{k}} \sum_{\underline{l}} |F_0(\underline{h}\underline{k}\underline{l})|^2 e^{2\pi \underline{i} \underline{h} \cdot \underline{r}}$$

Transforming to polar coordinates

$$P(\underline{r}, \underline{\delta}, \underline{\alpha}) = \frac{1}{V} \sum_{\underline{h}} \sum_{\underline{k}} \sum_{\underline{l}} |F_0^c|^2 e^{-\underline{i} \underline{s} \underline{r} \cos \delta}$$

Integrating the Patterson function over a spherical shell at a distance  $\underline{r}$  from the origin gives the number of interatomic distances of length  $\underline{r}$  weighted by the scattering powers of the atoms a distance  $\underline{r}$  apart; this function is  $4\pi \underline{r}^2 D(\underline{r})$ .

Where now

$$4\pi \underline{r}^2 D(\underline{r}) = \frac{1}{V} \int_0^{2\pi} \int_0^{\pi} \sum_{\underline{s}} |F_0^c|^2 e^{-\underline{i} \underline{s} \underline{r} \cos \delta} \underline{r}^2 \sin \delta d \delta d \alpha$$

$$4\pi \underline{r}^2 D(\underline{r}) = \frac{4\pi \underline{r}^2}{V} \sum_{\underline{s}} \left| \overset{\circ}{F}_{\underline{s}} \right|^2 \frac{\sin \underline{s} \underline{r}}{\underline{s} \underline{r}}$$

Separating out the  $\left| \overset{\circ}{F}_0 \right|^2$  term yields

$$4\pi \underline{r}^2 D(\underline{r}) = 4\pi \underline{r}^2 \left| \overset{\circ}{F}_0 \right|^2 + 4\pi \underline{r} \sum_{\substack{\underline{s} \neq 0 \\ \underline{s}}} \left| \overset{\circ}{F}_{\underline{s}} \right|^2 \sin \underline{s} \underline{r}$$

Figure 5 shows this summation. The peak at 1.35 Å has an area of 1254 electrons<sup>2</sup>.

The area, A, under a peak at  $\underline{r}$  Å is proportional to the number of distances of length  $\underline{r}$  and the product of the scattering of each of the atoms that are the distance  $\underline{r}$  apart. Therefore the area under the peak at 1.35 Å is given by the equation

$$A = 2n_1 \times n_2 \times m_1 \times m_2$$

$n_1$  = number of B-O distances per boron

$n_2$  = number of borons per unit cell

$m_1$  = number of electrons per boron

$m_2$  = number of electrons per oxygen

Assuming neutral atoms with  $m_1 = 5$ ,  $m_2 = 8$ , and  $n_2 = 6$ , the calculated number of B-O distances per boron is  $2.6 \approx 3$  within our limits of error. The limit of error on the area of the peaks is necessarily large for the following reasons: the small number of terms (44) in the summation,

cutting off the data at the  $\text{CuK}\alpha$  limit (the reflections at the  $\text{CuK}\alpha$  limit are still strong enough to indicate that there is considerably more data), and the uncertainty of the observed intensities.

Assuming that each boron has three oxygen neighbors then the area under the peak corresponds to  $m_1 = 4.07$ ,  $m_2 = 8.62$ , and consequently to a B-O bond with 31% ionic character, which is a reasonable value (24).

The  $1.35 \text{ \AA}$  B-O distance found agrees well with other compounds in which the boron has three oxygen neighbors in the same plane (25). Compounds in which the boron has four tetrahedral oxygen neighbors show B-O distances of about  $1.44 \text{ \AA}$  (26). Therefore the evidence indicates that the  $\text{B}_2\text{O}_3$  crystals probably contain planar  $\text{BO}_3$  triangles with the B-O distance  $1.35 \text{ \AA}$ . This result is in agreement with the results of Warren, Krutter and Morningstar (27) on  $\text{B}_2\text{O}_3$  glass. Their radial distribution sum (Fig. 6) for the  $\text{B}_2\text{O}_3$  glass is very similar to that for crystalline  $\text{B}_2\text{O}_3$  out to about  $3.0 \text{ \AA}$ , as would be expected if the immediate environment of the borons was the same in both forms.

RESULTS.  $\text{B}_2\text{O}_3$  crystallizes in a hexagonal structure with  $a_0 = 4.320 \text{ Kx.}$ ,  $c_0 = 8.319 \text{ Kx.}$ , and 3 molecules of  $\text{B}_2\text{O}_3$  in the unit cell, density  $2.42 \text{ g/cc.}$  Each boron is surrounded by a planar triangle with the B-O distance  $1.35 \text{ \AA}$ .

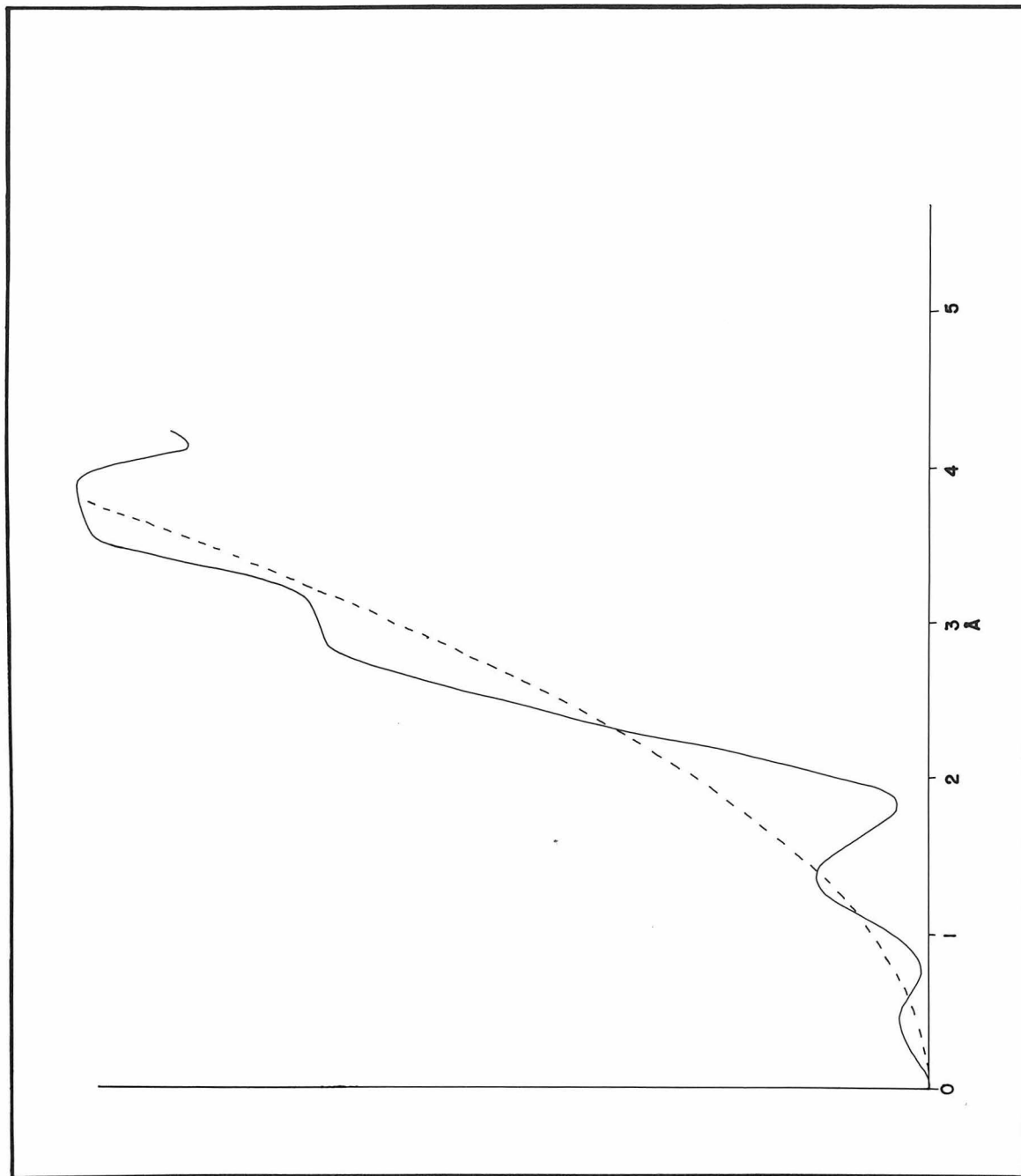
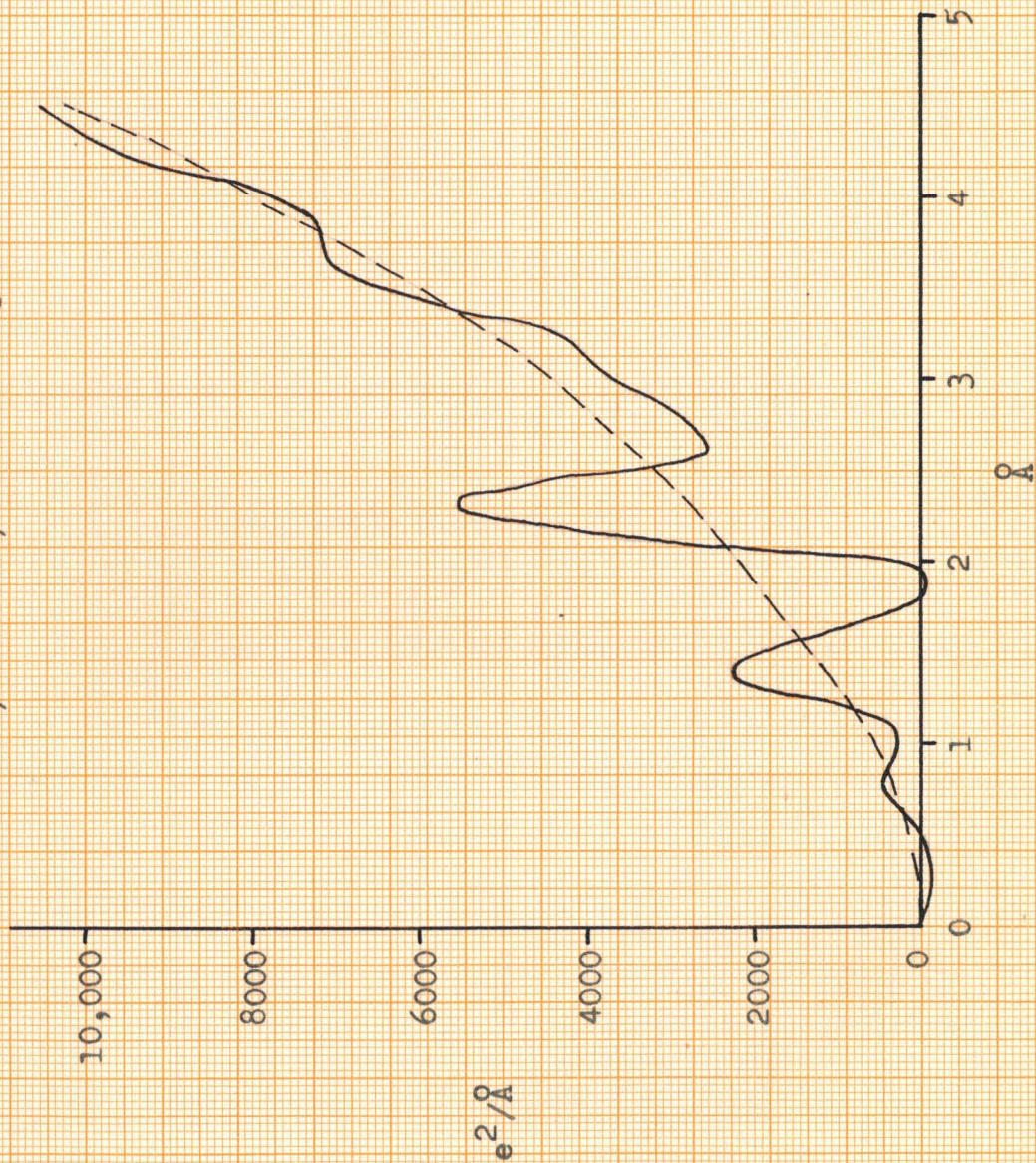


Figure 5

Radial Distribution Integral of  $B_2O_3$  Cryst.

Figure 6

From Warren, Krutter, and Morningstar (27)



Radial Distribution Integral of  $B_2O_3$  glass

PART B

THE ELECTRON DIFFRACTION INVESTIGATION  
OF  
SOME THREE-MEMBERED RINGS  
AND  
SOME HALOGENATED METHANES

INTRODUCTION. The present investigation of cyclopropane,  $C_3H_6$ , ethylene oxide,  $C_2H_4O$ , ethylene imine,  $C_2H_4NH$ , ethylene sulfide,  $C_2H_4S$ , and N-methyl ethylene imine was initiated by Dr. Henri Lévy, who prepared photographs of each of these five substances in 1938, made measurements of ring diameters on some of them, and calculated some theoretical intensity curves for cyclopropane and ethylene oxide. Subsequently Dr. Verner Schomaker measured all of the photographs and calculated radial distribution integrals. With the work reported in Section III the investigation has been brought to a conclusion.

Dr. Norman Davidson has been interested in the properties of some brominated methanes. One aspect of his investigations has been the varied reactivity of the bromine atom in these substances. At his suggestion the investigation reported in Section IV was undertaken. The primary object of the investigation was to determine the correlation, if any, between the carbon bromine distances and the reactivity of the bromine atom; however, it was also decided to determine out the complete structures. Trifluorobromomethane, difluorobromomethane, and difluorodibromomethane had not been investigated by electron diffraction previously. Trichlorobromomethane had been investigated but the reported C-Br distance of  $2.01 \text{ \AA}$ , considerably longer than any values for a C-Br distance reported recently (28) (the reported distances

average about 1.88 - 1.94 Å), made a redetermination desirable.

I wish to thank Dr. Davidson, Dr. Buchman, Dr. Eyster, and Dr. Sargent for furnishing the compounds used in these investigations.

The previous investigations of cyclopropane, ethylene oxide and trichlorobromomethane will be discussed in the sections dealing with those compounds.

EXPERIMENTAL. The electron diffraction equipment used in these investigations has been described by Brockway (29). Photographs of cyclopropane, ethylene oxide, ethylene imine, ethylene sulfide, and N-methyl ethylene imine were taken by Dr. Henri Lévy about ten years ago. The wave length value to be used with these photographs seemed doubtful so further photographs of cyclopropane and ethylene oxide were made in the course of this present work ( $\lambda = 0.0608$  Kx. by calibration with ZnO smoke (30)) and compared with the old photographs. An adjustment of the wave length value for the earlier photographs was found to be necessary in order to obtain agreement between the measurements of ring diameters between the two sets of photographs. The adjustment will be discussed in the section dealing with cyclopropane. When the original visual curves were drawn the value of the wave length used by Dr. Lévy ( $\lambda = 0.0613$ ) was assumed.

Photographs of the halogenated methanes were made with a camera distance of 10.90 cm and a wave length of 0.0605 Kx. calibrated against zinc oxide smoke (30).

INTERPRETATION. The visual curves were drawn in accordance with our observations and the expected general behavior of  $I(q)$  (Equation II). The radial distribution integrals were calculated from the visual interpretations with the equation

(I)

$$\underline{r} \underline{D}(\underline{r}) = \int_{\underline{q}=1,2,\dots}^{\underline{q} \text{ max}} I(\underline{q}) e^{-\underline{a}q^2} \sin \frac{\pi \underline{r}q}{10}$$

$$\underline{q} = \frac{40}{\lambda} \sin \frac{\delta}{2} = \frac{10}{\pi} \underline{s}$$

$\delta$  = scattering angle

where  $\underline{a}$  was determined so that  $e^{-\underline{a}q^2}$  was equal to 0.1 at  $\underline{q}$  max. The values of  $I(\underline{q})$  were taken from the visual curves. Theoretical intensity curves were calculated with the simplified theoretical scattering equation

(II)

$$I(\underline{q}) = \sum_{\underline{i} \neq \underline{j}} \sum \frac{\underline{Z}_{\underline{i}} \underline{Z}_{\underline{j}}}{\underline{r}_{\underline{i}\underline{j}}} e^{-\underline{b}_{\underline{i}\underline{j}} q^2} \sin \frac{\pi \underline{r}q}{10}$$

where the temperature factor  $\underline{b}$  was given the usual values 0.00016 for the C-H bonded distances, 0.00015 for the C...C in N-methyl ethylene imine and 0.0003 for all unbonded hydrogen distances. No other terms were temperature factored. All punched card (31) calculations were made with IBM machines.

The limits of error were estimated from the range of models that were acceptable qualitatively and had acceptable  $\frac{\underline{q}_c}{\underline{q}_0}$  values; the quality of the measurements as shown by the average deviation of  $\frac{\underline{q}_c}{\underline{q}_0}$  values; and an estimate of the magnitude of systematic errors such as deviations in wave length, uncertainty in calibration, and measurement of the camera distance.

III. THE THREE-MEMBERED RINGS  
Cyclopropane, Ethylene Oxide, Ethylene Imine,  
Ethylene Sulfide, and N-Methyl Ethylene Imine

VISUAL INTERPRETATION. The visual interpretation of the photographs of cyclopropane (V, Fig. 8), ethylene imine (V, Fig. 10), ethylene oxide (V, Fig. 12), and N-methyl ethylene imine (V, Fig. 13) was done simultaneously. These photographs have features which are only subtly different and are therefore subject to a differential interpretation of greater than usual accuracy. Of particular interest is the first minimum, which has a strong feature on the outside in cyclopropane, a weaker one on the outside in ethylene imine, and none in ethylene oxide. The feature is as strong in the N-methyl ethylene imine diffraction pattern as in that of cyclopropane but it has moved much further down into the minimum. The second maximum was observed to become broader and the third maximum narrower going in the sequence N-methyl ethylene imine--cyclopropane--ethylene imine--ethylene oxide. The sixth maxima were observed to be consistently weak and quite broad. The third minima and fourth maxima of the patterns of cyclopropane, ethylene imine, and ethylene oxide were especially useful. In cyclopropane the third minimum was observed to be very sharp as compared to the fourth maximum; in ethylene imine the minimum is broader but still not as broad as the fourth maximum; in the pattern

of ethylene oxide these features were observed to be anti-symmetrical. In other respects the photographs of these four compounds were observed to be very similar.

The notable features of the visual interpretation of ethylene sulfide are the asymmetry and broadness of the second maximum, the relative strength of the third and fifth minima, and the very strong sixth maximum.

CYCLOPROPANE, C<sub>3</sub>H<sub>6</sub>. Previous electron diffraction investigations have been made by Pauling and Brockway (32), and by Bastiansen and Hassel (33). Raman and infra-red spectra (34) show a D<sub>3h</sub> symmetry. Pauling and Brockway report C-C 1.53 Å and C-H 1.09 Å, and assumed the HCH angle to be 109°28'. Their radial distribution sum shows a peak due to the unbonded C...H distance from 2.2 - 2.5 Å. These values make an HCH bond angle of more than 125° improbable. The work of Bastiansen and Hassel has come to my attention only in abstract form with reported parameters of C-C 1.54 Å, C-H 1.08 Å, and HCH angle 118.2°.

Our doubts in regard to the wave length to be used with the old photographs made it necessary to estimate a more accurate value than the one, 0.0613 Kx., used by Dr. Lévy. The factors which lead to our doubts are the following:

1. No calibration of the wave length was made between the time the photographs were taken and the time the equipment was

transferred to its present location; 2. the lattice spacing of the gold foil used for wave length calibrations at the time the pictures were taken was shown to be in error by Malmberg and Lu (30); and 3. no shrinkage correction was made. The latter correction is perhaps not quite as serious if the calibration pictures and the experimental pictures have similar histories. In this case, however, the experimental pictures had aged and dried over a period of nine years before the measurements were made. Table A permits a correlation between the  $q_0$  values of Dr. Schomaker ( $S_1$ ) and of the author ( $P_1$ ) on the old pictures ( $\lambda = 0.0613$  Kx. assumed), and those of Dr. Schomaker ( $S_2$ ) and of the author ( $P_2$ ) on the new films ( $\lambda = 0.0608$  Kx.). Table A<sub>1</sub> permits a similar correlation between  $P_1$  and  $P_2$  for ethylene oxide. In order to obtain agreement in the average the old  $q_0$  values must be divided by 0.9922, corresponding to a corrected wave length of 0.0608 Kx. ( $0.9922 \times 0.0613$  Kx.). For the average  $q_0$  values reported in Tables VI, VII, VIII, IX, and X this correction has been made; for cyclopropane and ethylene oxide, of course, the effect is to make the size determination essentially independent of the old pictures.

The radial distribution integral R (Fig. 8) calculated from the visual interpretation, V (Fig. 8), indicates bonded distances of 1.10 Kx. (C-H) and 1.52 Kx. (C-C), and a non-bonded C...H distance of 2.24 Kx., corresponding to an HCH

Table A

<u>S<sub>1</sub></u>	<u>S<sub>2</sub></u>	<u>P<sub>1</sub></u>	<u>P<sub>2</sub></u>	<u><math>\frac{S_1}{S_2}</math></u>	<u><math>\frac{P_1}{P_2}</math></u>
18.61	18.48	19.27	19.13	1.0070	1.0073
23.46	23.42	23.26	23.68	1.0017	0.9823
29.17	28.58	29.22	29.17	1.0206	1.0017
34.23	34.23	33.54	34.32	1.0000	0.9773
48.99	49.08	48.45	49.55	0.9982	0.9778
55.10	55.64	55.54	56.20	0.9903	0.9883
61.70	61.87	61.50	61.91	0.9973	0.9935
68.52	69.07	68.85	69.76	0.9920	0.9870
74.62	76.30	75.35	75.62	0.9780	0.9964
81.47	84.03	82.12	82.87	0.9695	0.9909
Average correction				0.9955	0.9903

Table A<sub>1</sub>

<u>P<sub>1</sub></u>	<u>P<sub>2</sub></u>	<u><math>\frac{P_1}{P_2}</math></u>
30.47	30.15	1.0106
36.10	36.12	0.9994
44.57	44.95	0.9915
50.31	51.82	0.9709
58.25	57.78	1.0081
64.15	64.97	0.9874
72.07	72.21	0.9981
77.86	78.70	0.9893
84.98	85.38	0.9953
89.56	91.83	0.9753
96.25	98.97	0.9725
Average correction		0.9907

bond angle of  $116^\circ$ . Theoretical intensity functions (Figs. 7 & 8) were calculated for a systematic range of molecular shapes in the neighborhood of the shape indicated by the radial distribution function with the C-H distance taken as 1.09 Kx. for all models. The acceptable models lie in the ellipse (Fig. 7). Curve G is the curve corresponding to the model of Bastiansen and Hassel. Curves B3 and B4 are the only curves on which the region from the second to the fifth maximum is satisfactory. B4 has the third minimum deeper than desirable but it is not possible to eliminate B4 on this basis. After the necessary scale change the final parameters and estimated limits of error are C-C  $1.515 \pm 0.02$  Kx., C-H  $1.10 \pm 0.03$  Kx., HCH angle  $116 \pm 5^\circ$ , and C...H  $2.24 \pm 0.06$  Kx. The agreement between observed and calculated  $\underline{q}$  values is shown for this best model in Table VI and in Table VI<sub>a</sub> for the model with the parameter values reported by Bastiansen and Hassel, which lie just outside our limits of error.

The bracketed  $\underline{q}$  values were not included in determining the averages  $\frac{\underline{q}_c}{\underline{q}_o}$  and the corresponding average deviations on account of the relative inaccuracy of measuring broad features and features near the center of the diffraction pattern.

The calculated moment of inertia,  $I_B$ , for the best model (Table VI) is  $42.4 \times 10^{-40}$  g-cm<sup>2</sup>, in fairly satisfactory

Figure 7

	$\frac{C-C}{C-H}$	$\frac{1.55}{1.09}$			$\frac{1.52}{1.09}$			$\frac{1.49}{1.09}$
$\angle$ HCH								
105°		A1			B1			C1
-								
-								
110		A2			B1''			C2
-								
-								
115		A3			B3			C3
-								
-								
120		A4			B4			C4
-								
-								
125		A5			B5			C5

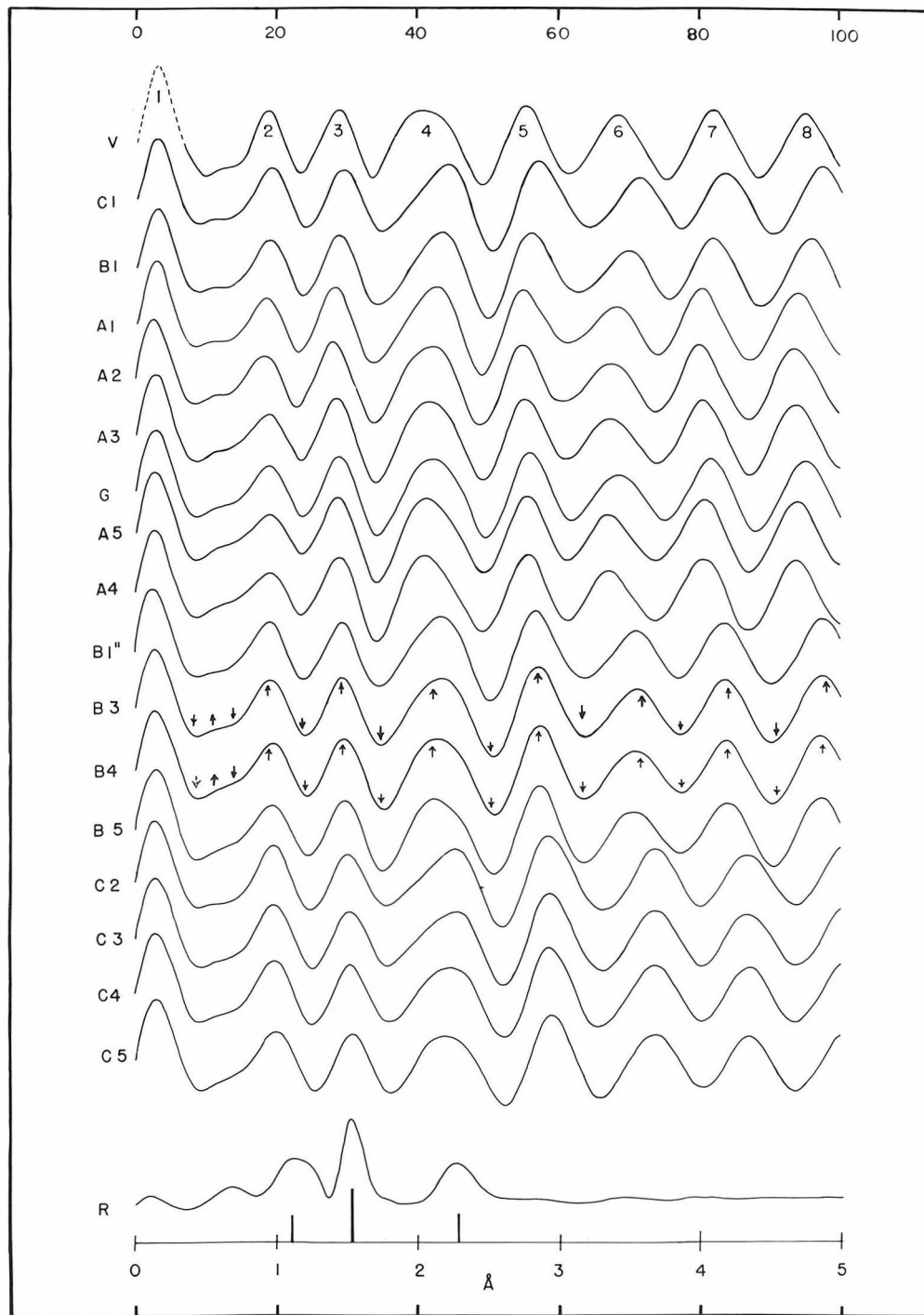


Figure 8

Cyclopropane

Table VICyclopropane

C-C = 1.515 Kx.

C-H = 1.10 Kx.

 $\angle\text{HCH} = 116^\circ$ 

<u>Max.</u>	<u>Min.</u>	<u>q<sub>o</sub></u>	<u>q<sub>c</sub></u>	<u><math>\frac{q_c}{q_o}</math></u>
	1	( 8.74)	( 8.90)	--
2a		(11.05)	(10.90)	--
	2a	(14.24)	(13.68)	--
2		18.92	19.1	1.0095
	2	23.52	23.49	0.9987
3		29.15	29.04	0.9962
	3	34.05	34.39	1.0100
4		(41.79)	(43.11)	--
	4	49.36	49.63	1.0055
5		56.30	56.49	1.0034
	5	62.20	61.74	0.9926
6		69.59	70.56	1.0139
	6	76.61	76.80	1.0025
7		83.32	82.59	0.9912
	7	89.39	89.34	0.9994
8		96.98	96.52	0.9953
			Average	1.0015
			Average deviation	0.60%

Table VI<sub>a</sub>Cyclopropane

C-C = 1.54 Kx.

C-H = 1.08 Kx.

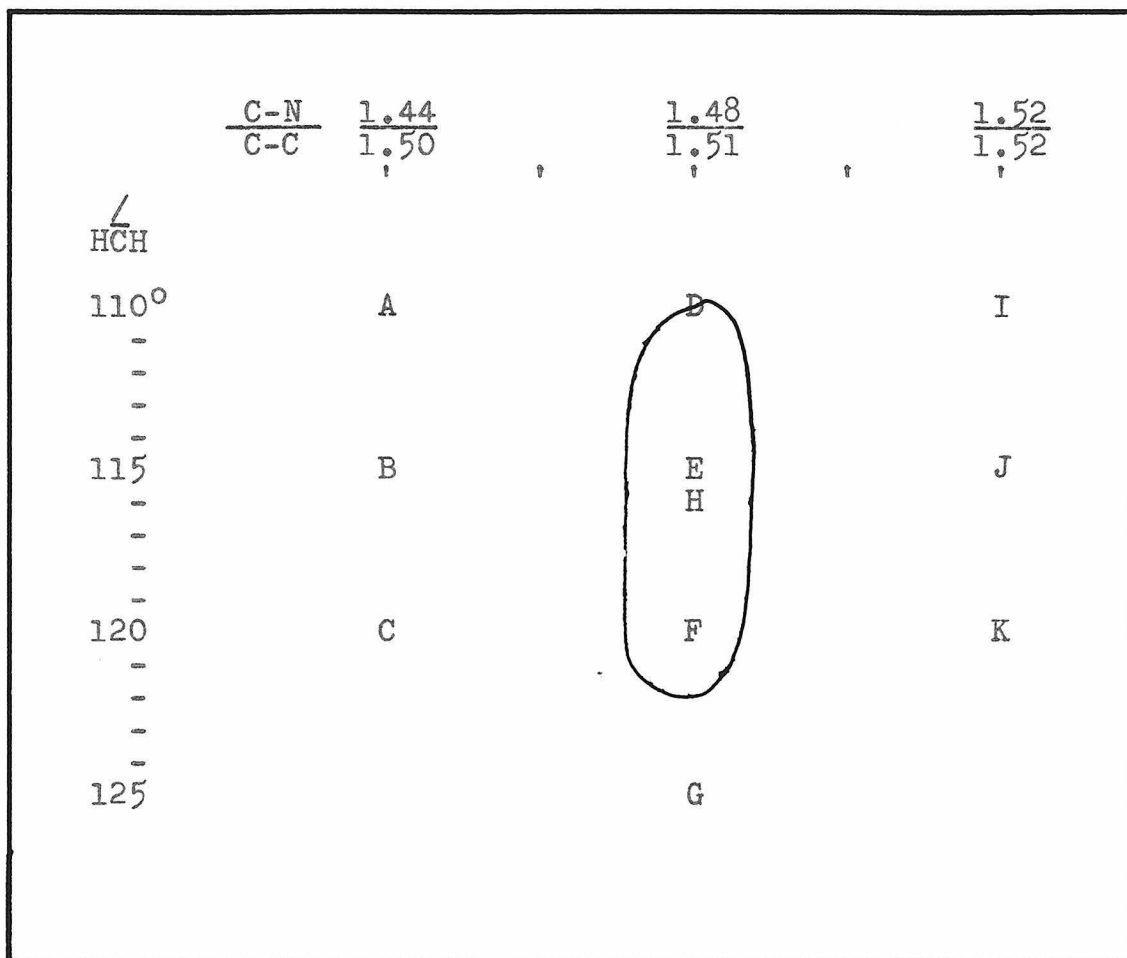
 $\angle\text{HCH} = 118^\circ$ 

<u>Max.</u>	<u>Min.</u>	<u>q<sub>o</sub></u>	<u>q<sub>c</sub></u>	<u><math>\frac{q_c}{q_o}</math></u>
	1	( 8.74)	( 9.01)	--
2a		(11.05)	(11.07)	--
	2a	(14.24)	(14.74)	--
2		18.92	18.92	1.0000
	2	23.52	23.60	1.0034
3		29.15	28.74	0.9859
	3	34.05	34.47	1.0123
4		(41.79)	(41.77)	--
	4	49.36	49.62	1.0053
5		56.30	55.71	0.9895
	5	62.20	61.65	0.9912
6		69.59	67.69	0.9727
	6	76.61	74.48	0.9722
7		83.32	81.17	0.9742
	7	89.39	87.57	0.9796
8		96.98	94.31	0.9725
Average				0.9882
Average deviation				1%

agreement with the spectroscopic value of  $41.9 \times 10^{-40} \text{ g-cm}^2$  (34,35). Scaling our model down by an amount (0.6%) well within our limits of error would make the agreement exact. The model with the values of the parameters as reported by Bastiansen and Hassel has a calculated  $I_B$  of  $42.9 \times 10^{-40} \text{ g-cm}^2$ , a discrepancy of 2.4%.

ETHYLENE IMINE,  $C_2H_4NH$ . The radial distribution integral, R (Fig. 10), calculated from the visual interpretation, V (Fig. 10), indicates bonded distances for the average of 4 C-H and 1 N-H of 1.08 Kx., and for the average of 2 C-N and 1 C-C of 1.50 Kx. The broad peak centered at 2.20 Kx. contains the unbonded C...H and N...H distances. Theoretical intensity curves (Figs. 9 & 10 show some representative curves) were calculated assuming that the HCH plane bisects the CCN angle and that the N-H bond is symmetrical and makes a  $58^\circ$  angle with the plane of the ring. The average and the ratio of the C-C and C-N distances and the HCH bond angle were varied systematically around a model with C-C 1.52 Kx., C-N 1.47 Kx. and an HCH bond angle  $116^\circ$ . The C-H distance was taken as 1.09 Kx. and the N-H as 1.01 Kx. for all models. Models D, E, H, and F (Figs. 9 & 10) are acceptable. E and H are the most desirable because the region from the second maximum to the fourth minimum is very similar to the region as interpreted from the photographs.

Figure 9



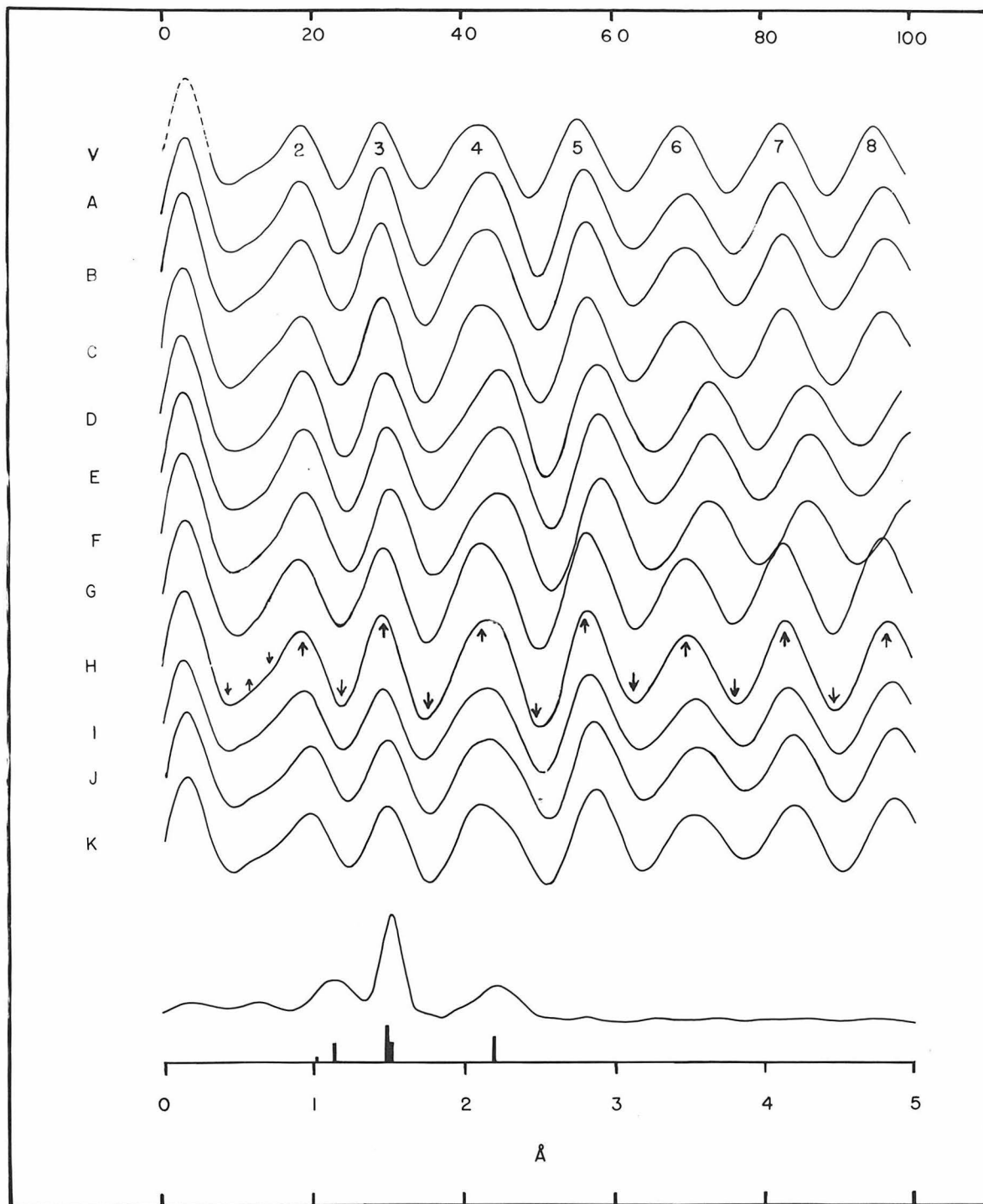


Figure 10

Ethylene Imine

Table VII

Ethylene Imine

C-C = 1.52 Kx., C-N = 1.49 Kx., C-H = 1.10 Kx.,  
 N-H = 1.01 Kx.,  $\angle$ HCH = 116°,  $\angle$ CNH = 117°

<u>Max.</u>	<u>Min.</u>	<u>q<sub>o</sub></u>	<u>q<sub>c</sub></u>	<u><math>\frac{q_c}{q_o}</math></u>
	1	( 8.3)	( 9.7)	--
2a		(11.6)	(11.1)	--
	2a	(14.20)	(13.60)	--
2		18.64	18.44	0.9893
	2	23.78	23.68	0.9958
3		29.68	29.43	0.9915
	3	35.37	35.47	1.0028
4		(42.63)	(43.13)	--
	4	49.58	50.09	1.0102
5		56.18	56.74	1.0099
	5	62.54	63.29	1.0121
6		70.04	70.04	1.0000
	6	76.09	76.39	1.0040
7		82.70	82.94	0.9964
	7	88.69	88.38	0.9966
8		95.74	96.45	1.0074

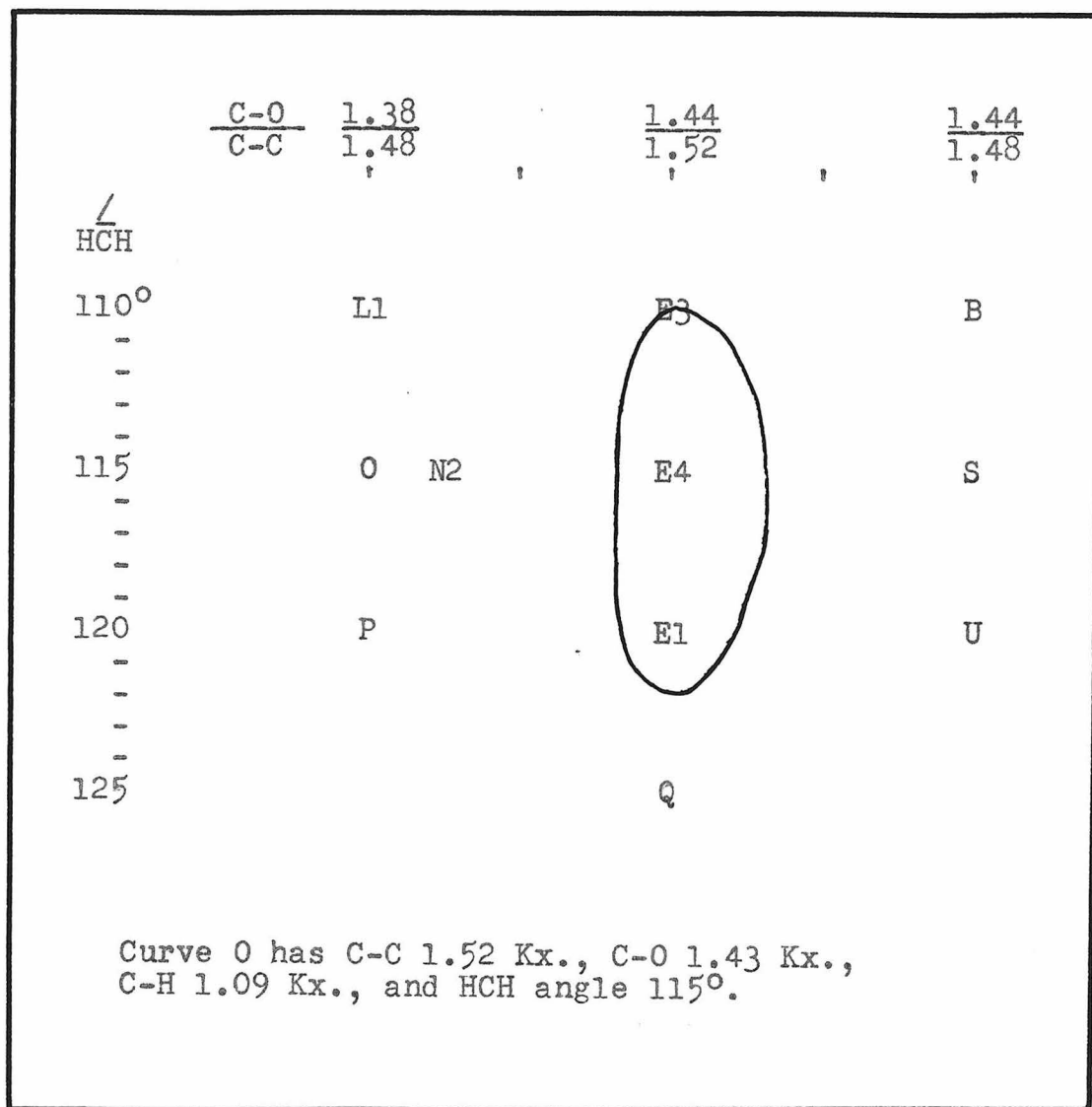
Average 1.0013

Average deviation 0.64%

The theoretical curves proved insensitive to changes in the ratio of the  $\frac{C-C}{C-N}$  distance but a ratio of less than 0.93 is unacceptable. Ratios of  $\frac{C-N}{C-C} > 1$  were not investigated. The average of C-C and C-N is  $1.50 \pm 0.02$  Kx.; assuming that C-C is 1.52 Kx. the C-N is  $1.49 \pm 0.02$  Kx. The final results are C-C 1.52 Kx. (assumed), C-N  $1.49 \pm 0.02$  Kx., C-H  $1.10 \pm 0.04$  Kx., and HCH bond angle  $116 \pm 6^\circ$ . Table VII shows the agreement between observed and calculated  $q$  values for the best model.

ETHYLENE OXIDE. A previous investigation of ethylene oxide has been made by Ackermann and Mayer (36). The purpose of the investigation was to prove the ring structure; no attempt was made to determine the parameters accurately. The radial distribution integral, R (Fig. 12), calculated from the visual interpretation, V (Fig. 12), indicates bonded distances of C-H 1.10 Kx. and the average C-O and C-C 1.47 Kx., and unbonded C...H and O...H distances averaging 2.17 Kx. Theoretical intensity curves (Figs. 11 & 12 show some representative curves) were calculated with C-H 1.09 Kx. for all models and assuming that the HCH plane bisects the CCO angle. The C-O and C-C distances and their ratio were varied systematically around 1.43 Kx. and 1.52 Kx., respectively, and the HCH angle was varied around the value found for cyclopropane,  $116^\circ$ .

Figure 11



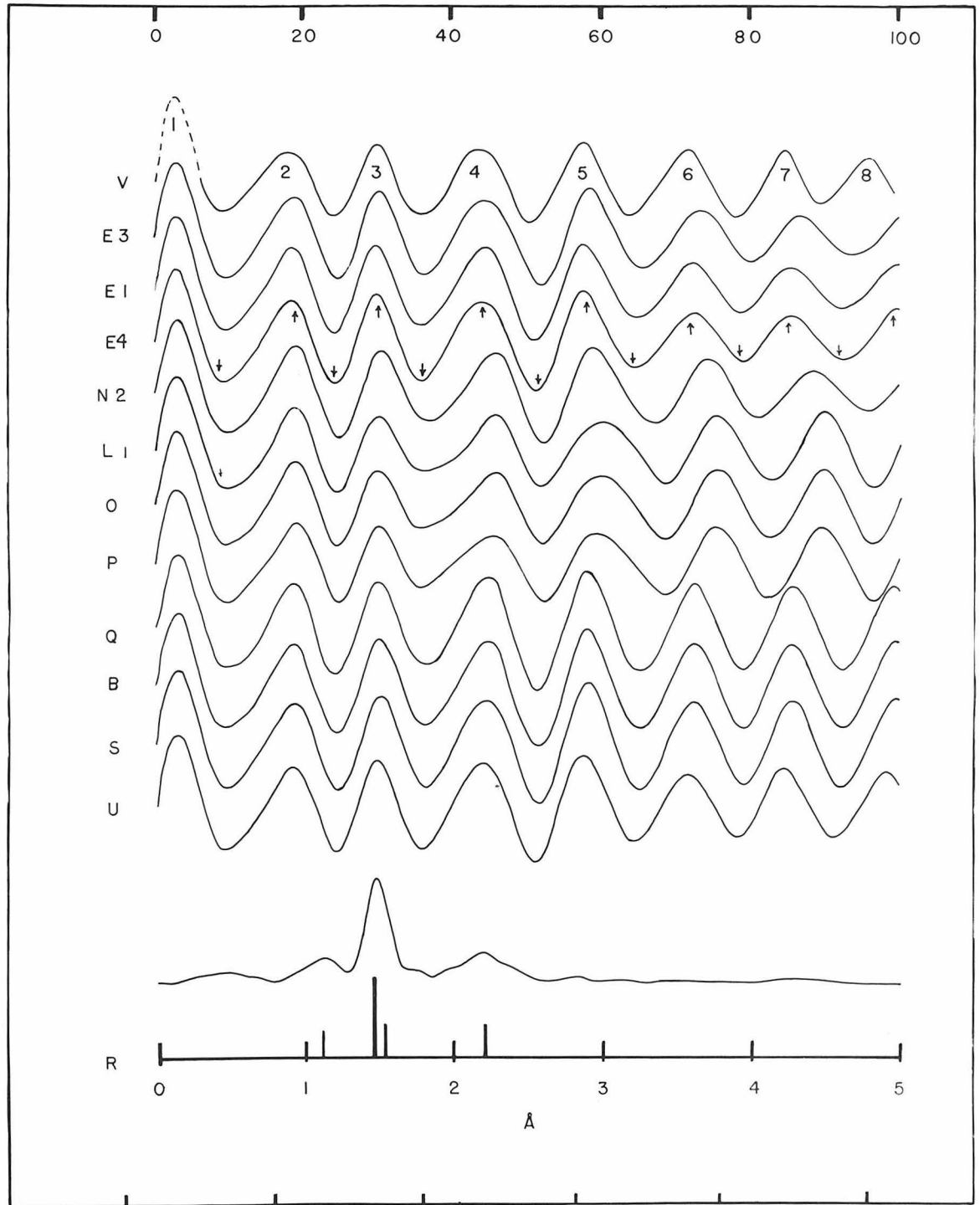


Figure 12

Ethylene Oxide

Table VIII

Ethylene Oxide

C-C = 1.52 Kx., C-O = 1.45 Kx., C-H = 1.10 Kx.,  $\angle$ HCH = 116°

<u>Max.</u>	<u>Min.</u>	<u>q<sub>o</sub></u>	<u>q<sub>c</sub></u>	<u><math>\frac{q_o}{q_c}</math></u>
	1	( 8.9)	( 9.5)	--
2		(19.1)	(18.6)	--
	2	22.28	24.49	1.0083
3		30.43	30.13	0.9901
	3	36.48	36.43	0.9986
4		44.49	44.54	1.0011
	4	50.89	51.40	1.0099
5		58.45	57.90	0.9905
	5	64.70	64.90	1.0031
6		72.36	72.16	0.9972
	6	78.71	78.81	1.0013
7		85.46	85.21	0.9971
	7	93.55	92.21	0.9857
8		99.74	99.27	0.9953

Average 0.9982

Average deviation 0.55%

Acceptable models were found with  $\frac{C-O}{C-C}$  ratios down to 0.93; ratios greater than 1 were not investigated. The models N2, E4, and S were acceptable with E4 being the best. Assuming the C-C distance to be 1.52 Kx. the C-O distance is  $1.45 \pm 0.02$  Kx. and the average of the C-O and C-C distance is  $1.47 \pm 0.02$  Kx. The final results are C-C 1.52 Kx. (assumed), C-O  $1.45 \pm 0.02$  Kx., and HCH angle  $116 \pm 6^\circ$ . Table VIII shows the agreement between observed and calculated  $q$  values for the best model.

N-METHYL ETHYLENE IMINE. The radial distribution integral, R (Fig. 13), calculated from the visual interpretation, V (Fig. 13), indicates bond distances for C-H of 1.09 Kx., and the average of C-C and C-N of 1.49 Kx., unbonded distance for the average of C...H and N...H of 2.19 Kx. and for C...C of 2.48 Kx. Theoretical models (Fig. 13), for which the assumption was made that the ring has the configuration found for the ring in ethylene imine, were calculated. Models A, B, and C have methyl-nitrogen distances of 1.47 Kx. and the angle of the methyl group with the ring  $57.5^\circ$ ,  $58.5^\circ$ , and  $59.5^\circ$ , respectively. Model B is the only model on which the sixth maximum is satisfactory. Models D and E have  $CH_3$ -N distances of 1.44 and 1.50, respectively. A wider range of models was calculated in an attempt to find other regions of acceptability but with no success.

Table IX

N-Methyl Ethylene Imine

Ring as in  $C_2H_4NH$ ,  $C_{CH_3}-N = 1.47$  Kx.,  $\angle CNC_{CH_3} = 116^\circ$

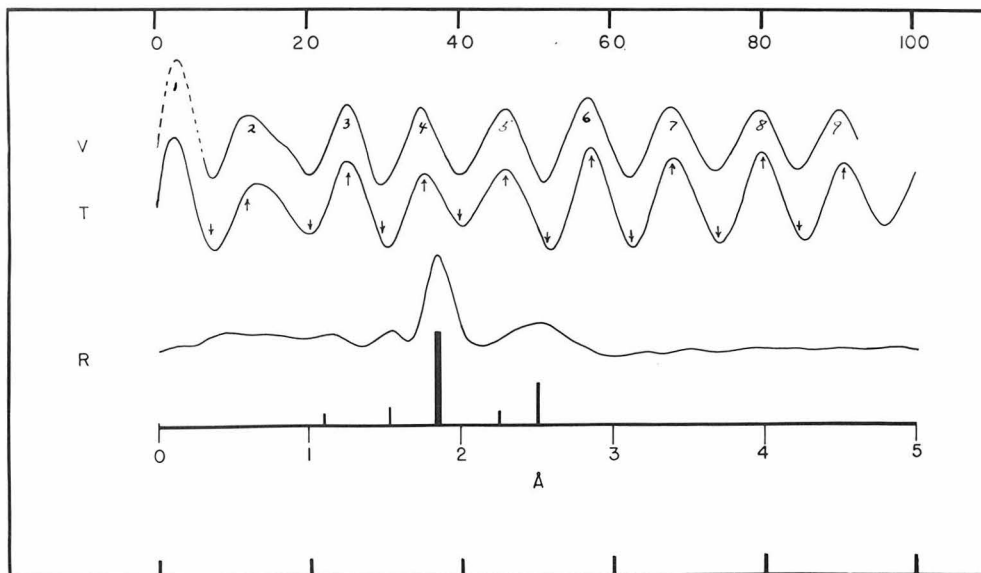
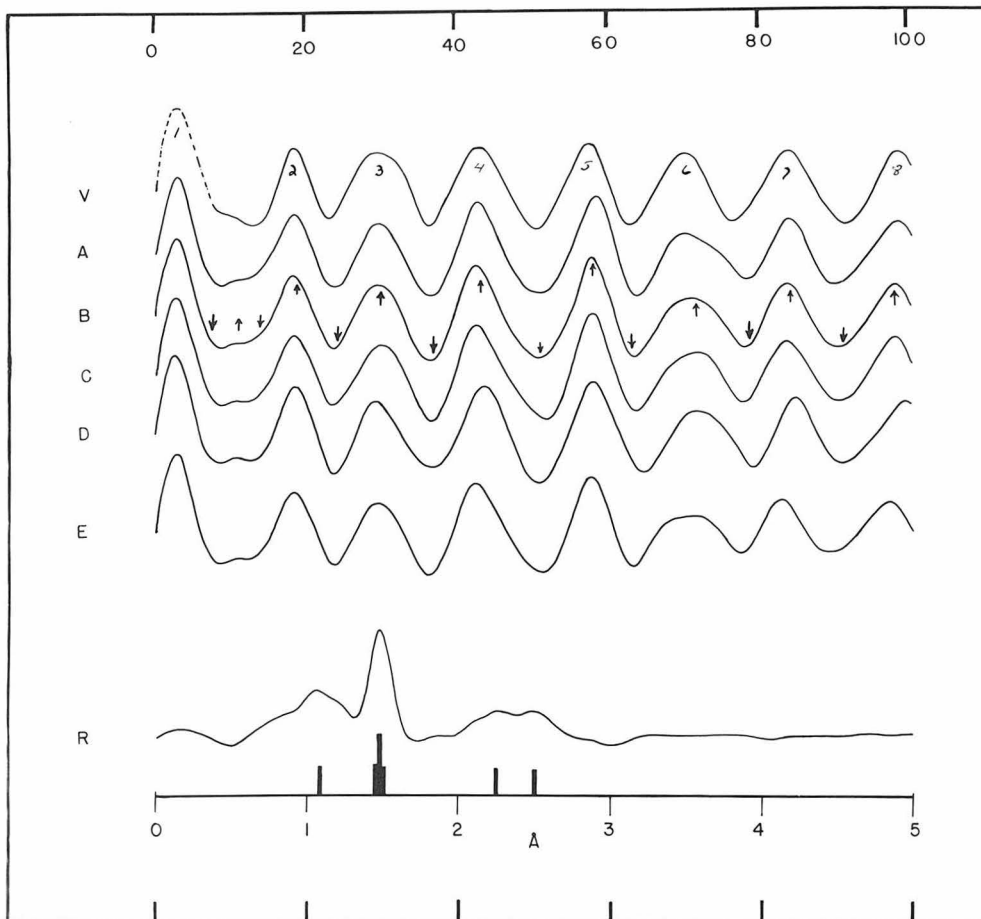
<u>Max.</u>	<u>Min.</u>	<u>q<sub>o</sub></u>	<u>q<sub>c</sub></u>	<u><math>\frac{q_c}{q_o}</math></u>
	1	( 7.05)	( 9.07)	--
1a		(10.58)	(10.98)	--
	1a	(12.80)	(12.90)	--
2		18.54	18.54	1.0000
	2	23.38	23.73	1.0151
3		29.98	29.88	0.9963
	3	36.78	36.78	1.0000
4		43.59	43.03	0.9873
	4	51.10	51.60	1.0099
5		58.05	58.15	0.0017
	5	63.29	63.29	1.0000
6		71.25	71.55	1.0042
	6	77.35	78.31	1.0126
7		84.66	84.35	0.9964
	7	92.31	91.21	0.9880
8		98.51	98.46	0.9995

Average 1.0014

Average deviation 0.54%

Under the assumption that the ring configuration is that in ethylene imine the results indicate that the methyl group is at an angle of  $58.5 \pm 2^\circ$  to the ring and the nitrogen-methyl distance is  $1.47 \pm 0.04$  Kx. Table IX shows the agreement between observed and calculated  $\underline{q}$  values for the best model. This result is in accord with the prediction of Eyster (37) that the angle to the plane of the ring would be less than  $64^\circ$ .

ETHYLENE SULFIDE. The radial distribution integral, R (Fig. 14), calculated from the visual interpretation, V (Fig. 14), indicates distances of 1.10 Kx. (C-H), 1.52 Kx. (C-C), 1.82 Kx. (C-S), and 2.48 Kx. (S...H). Theoretical intensity curves were calculated with values of the parameters near the radial distribution values. The theoretical curves proved very insensitive to changes in the C-C, C-H and C...H distances. It was therefore only possible to determine the C-S and S-H distances. Curve T (Fig. 14) shows the most acceptable model with C-C 1.53 Kx. (assumed), C-H 1.10 Kx. (assumed),  $\angle\text{HCH } 116^\circ$  (assumed), C-S 1.82 Kx., and S...H 2.48 Kx. The final parameters determined with the limits of error are C-S  $1.82 \pm 0.02$  Kx., and S...H  $2.48 \pm 0.07$  Kx. Table X shows the agreement between observed and calculated  $\underline{q}$  values for the best model.



Figures 13 and 14

N-Methyl Ethylene Imine and Ethylene Sulfide

Table X

Ethylene Sulfide

C-S = 1.82 Kx., C-C = 1.53 Kx., C-H = 1.10 Kx.,  $\angle$ HCH = 116°

<u>Max.</u>	<u>Min.</u>	<u>q<sub>o</sub></u>	<u>q<sub>c</sub></u>	<u><math>\frac{q_c}{q_o}</math></u>
	1	7.26	7.86	--
2		11.90	13.50	--
	2	14.20	--	--
3		17.53	--	--
	3	20.41	20.26	0.9926
4		25.50	25.30	0.9921
	4	29.68	30.28	1.0204
5		35.58	35.37	0.9943
	5	40.11	40.51	1.0100
6		46.31	46.36	1.0011
	6	51.50	51.85	1.0068
7		57.60	57.39	0.9965
	7	62.63	62.79	1.0024
8		68.29	68.43	1.0022
	8	74.33	74.07	0.9966
9		80.37	79.87	0.9937
	9	85.01	85.46	1.0053
10		91.00	90.75	0.9972

Average 1.0008

Average deviation 0.61%

DISCUSSION. The structures of these three-membered rings indicate that the strain caused by the small bond angle in the ring is distributed almost equally between the other angles. The six carbon bond angles in these compounds have values of about  $60^\circ$ ,  $116^\circ$ , and four  $117^\circ$ . Changes of only 0.0025 Kx. in the unbonded hydrogen distance would make the latter five all equal. This change makes no observable change in the diffraction pattern. The  $\text{CH}_3$  group in N-methyl ethylene imine has a  $58.5^\circ$  angle with the plane of the ring which, if the electron pair can be considered a group, makes the nitrogen bond angles about  $61^\circ$ ,  $117^\circ$ , and four  $116^\circ$ .

The short C-C distance of 1.515 reported in cyclopropane is in agreement with the value 1.52 Kx. Pauling and Brockway (32) reported for the C-C peak in their R.D.I. The first five rings, which are all they observed, are sensitive to the average of the C-C and C-H distance but rather insensitive to the ratio. As a result a 1.52 Kx. C-C and 1.10 Kx. C-H would fit the observations of Pauling and Brockway as well as the 1.53 Kx. C-C and 1.09 Kx. C-H upon which they decided. With the observation of three additional rings it is possible to determine the C-C/C-H ratio more accurately. This evidence indicates that the C-C distance in cyclopropane is definitely shorter than the normal value for alkanes, 1.54 Kx.

Several theoretical calculations (38) of the HCH bond angle have been made. Coulson and Moffitt predict an HCH angle of  $113^\circ$  and a shortening of the C-C distance; both results are in general agreement with this investigation. The  $121^\circ$  angle calculated by Kilpatrick and Spitzer is improbable on the basis of our results.

The original article by Bastiansen and Hassel (33) has been made available since the rest of the thesis was written. They report the following parameters: C-C =  $1.535 \text{ \AA}$  (in a footnote), C-H =  $1.08 \text{ \AA}$ , HCH angle  $118.2^\circ$ , and CCH angle  $116.2^\circ$ , with a probable error in the angles of  $2^\circ$ . It is not clear to which angle this probable error refers; a  $2^\circ$  error in the CCH angle corresponds to an  $8^\circ$  error in the HCH angle. If that interpretation is correct a  $2^\circ$  reduction in the CCH angle would make the moment of inertia agree with the spectroscopic value. If the probable error in the HCH angle is  $2^\circ$  no such agreement can be obtained.

It is noteworthy in each of these compounds in which another atom, X, is substituted for one of the carbon atoms in the cyclopropane ring that the C-X distance seems to be lengthened over the sum of the covalent radii of carbon and X, viz. C-N,  $1.49 \text{ Kx.}$  (sum of covalent radii  $1.47 \text{ Kx.}$ ), C-O,  $1.45 \text{ Kx.}$  ( $1.43 \text{ Kx.}$ ), and C-S,  $1.82 \text{ Kx.}$  ( $1.81 \text{ Kx.}$ ). This trend is even more striking when compared with the short ( $1.515 \text{ Kx.}$ ) C-C distance found in cyclopropane. It is

certainly possible that the introduction of another atom in the ring lengthens all of the bonds. If the logical assumption had been made that the bond lengthening was distributed uniformly among the bonds in the ring, the results for ethylene oxide would be C-C 1.55 Kx. and C-O 1.44 Kx., and the results for ethylene imine would be C-C 1.55 Kx. and C-N 1.48 Kx. These values of the distances are completely acceptable on the basis of the determinations reported in this section.

RESULTS\*

Cyclopropane

$$\begin{aligned} \text{C-C} &= 1.515 \pm 0.02 \text{ Kx.} \\ \text{C-H} &= 1.10 \pm 0.025 \text{ Kx.} \\ \angle\text{HCH} &= 116 \pm 5^\circ \end{aligned}$$

Ethylene Imine

$$\begin{aligned} \text{C-C} &= (1.52 \text{ Kx.}) \\ \text{C-N} &= 1.49 \pm 0.02 \text{ Kx.} \\ \text{C-H} &= 1.10 \pm 0.03 \text{ Kx.} \\ \angle\text{HCH} &= 116 \pm 6^\circ \\ \text{Average C-C and C-N} &= 1.50 \pm 0.02 \text{ Kx.} \\ \text{H-N} &= (1.01 \text{ Kx.}) \\ \angle\text{CNH} &= (116^\circ) \end{aligned}$$

Ethylene Oxide

$$\begin{aligned} \text{C-C} &= (1.52 \text{ Kx.}) \\ \text{C-O} &= 1.45 \pm 0.02 \text{ Kx.} \\ \text{C-H} &= 1.10 \pm 0.03 \text{ Kx.} \\ \text{Average C-C and C-O} &= 1.47 \pm 0.02 \text{ Kx.} \\ \angle\text{HCH} &= 116 \pm 6^\circ \end{aligned}$$

Ethylene Sulfide

$$\begin{aligned} \text{S}\cdots\text{H} &= 2.48 \pm 0.07 \text{ Kx.} \\ \text{C-S} &= 1.82 \pm 0.02 \text{ Kx.} \\ \text{C-C} &= (1.52 \text{ Kx.}) \\ \angle\text{HCH} &= (116^\circ) \end{aligned}$$

N-Methyl Ethylene Imine

$$\begin{aligned} &(\text{Ring configuration as in ethylene imine}) \\ \angle\text{CHCCH}_3 &= 116^\circ \\ \text{CCH}_3\text{-N} &= 1.47 \pm 0.04 \text{ Kx.} \end{aligned}$$

---

\* Values in parentheses are assumed.

IV. THE HALOGENATED METHANES  
Difluorobromomethane, Trifluorobromomethane,  
Trichlorobromomethane, and Difluorodibromomethane

VISUAL INTERPRETATION. The difluorobromomethane and trifluorobromomethane patterns (curve V, Figs. 16 & 18) are dominated by the Br-F term, both showing fourteen rings to  $q = 100$ . The other terms modulate the basic pattern but since they are of lower frequency do not have much effect upon the positions of the features. The determination of the shorter distances and the bond angles depends mainly, therefore, upon the estimation of the relative strengths of the maxima and minima. The early parts of the curves,  $q < 50$ , are insensitive to the weaker distances.

The situation regarding the patterns of difluorodibromomethane and trichlorobromomethane is somewhat different. Each of these patterns has a pair of long, strong terms (F...Br and Br...Br, and Cl...Cl and Cl...Br, respectively) and neither pattern has a term of weight greater than the sum of the weights of all the other terms. The most striking observation on the photographs of trichlorobromomethane is the position where the Cl-Cl and Cl-Br distances beat against each other (V, Fig. 20), and the number of weak features before the terms are in phase again. The photographs of difluorodibromomethane were all rather light and the very sensitive region in the neighborhood of  $q = 65$  (V, Fig. 22)

was difficult to interpret; as a result the determination does not have the accuracy that could be obtained if it were possible to interpret this region unequivocally. The shape of the fourth maximum and the relation between the seventh and eighth minima also proved to be very structure sensitive. The available sample of  $\text{CF}_2\text{Br}_2$  was insufficient for making heavy pictures.

DIFLUOROBROMOMETHANE. The radial distribution integral, R (Fig. 16), indicates bonded distances of 1.34 Kx. (C-F) and 1.92 Kx. (C-Br) and unbonded distances of 2.20 Kx. (F...F) and 2.68 Kx. (Br...F). The C-H and F...H distances have too little weight to show on the R.D.I., and the Br...H peak falls under the Br...F peak. Theoretical intensity curves were calculated for different values of the ratio  $\frac{\text{Br-F}}{\text{Br-C}}$  and the FCBr and FCF angles. The C-H distance was assumed to be 1.09 Kx. and the hydrogen atom was assumed to be symmetrically located with respect to the halogen atoms. The Br-F distance was taken as 2.68 Kx. for all models. The curves proved insensitive to changes of  $5^\circ$  in the FCF angle from the tetrahedral value, making the attempt to determine this angle unfruitful. In the determination of the other parameters the FCF angle was therefore assumed to be tetrahedral. The theoretical curves (Figs. 15 & 16) proved to be quite sensitive to variations in the Br-C

distance and FCB<sub>r</sub> bond angle; only curve E was completely satisfactory, although D is just on the limit of acceptability.

Figure 15

	$\frac{\text{Br-F}}{\text{C-Br}}$	$\frac{2.68}{1.87}$		$\frac{2.68}{1.91}$		$\frac{2.68}{1.95}$
$\angle\text{FCBr}$						
107°		C		F		I
-						
109		B		E		H
-						
111		C		D		G

Difluorobromomethane therefore has  $\frac{\text{Br-F}}{\text{C-Br}} = 1.395 \pm 0.015$  and the FCB<sub>r</sub> angle =  $110 \pm 2^\circ$ . The final result is C-Br  $1.915 \pm 0.03$  Kx., C-F  $1.35 \pm 0.04$  Kx., Br-F  $2.68 \pm 0.02$  Kx., FCF angle  $109.5^\circ$  (assumed), and FCB<sub>r</sub> angle  $110 \pm 2^\circ$ . Table XI shows the agreement between observed and calculated q values for the final model.

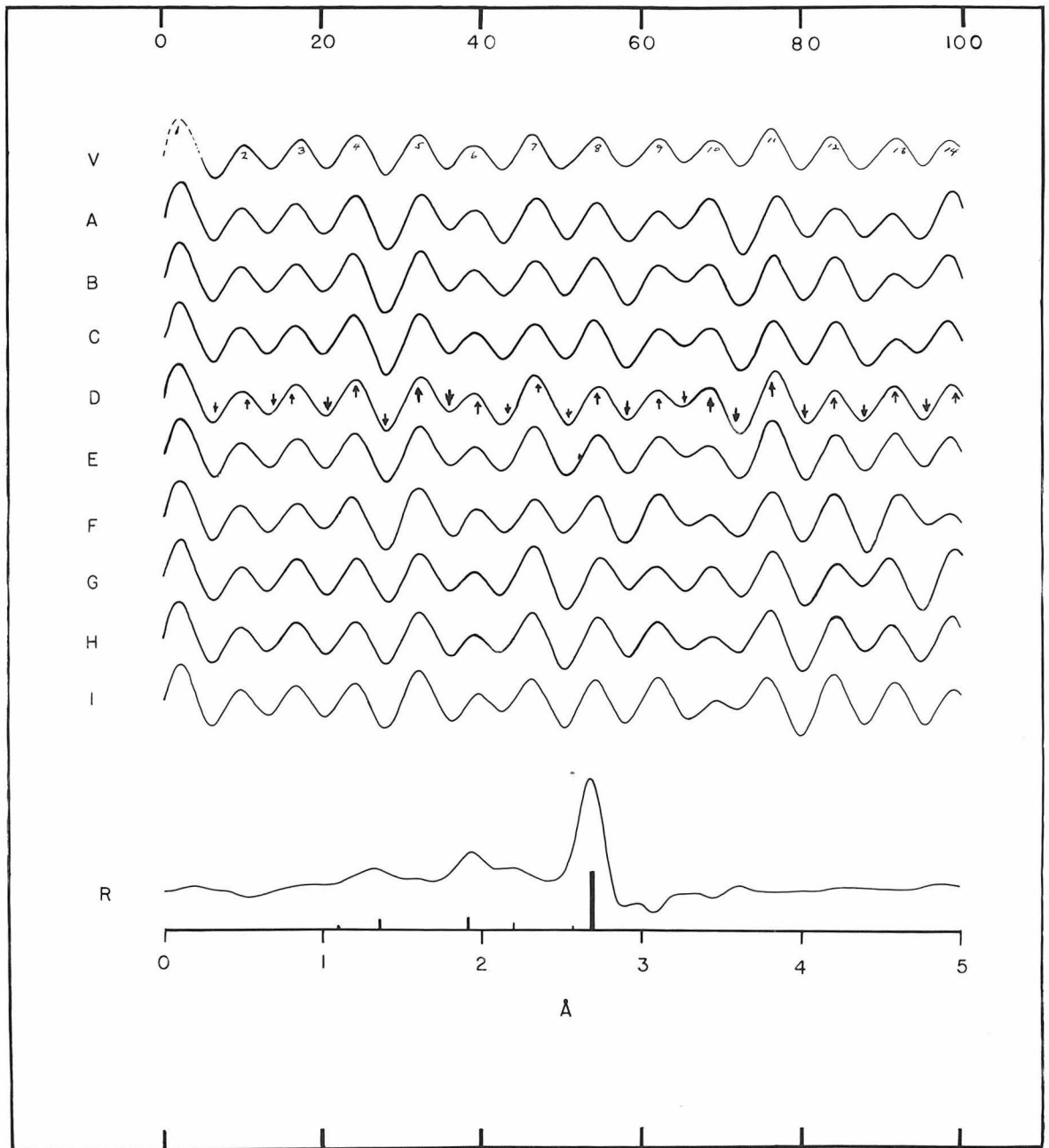


Figure 16

Difluorobromomethane

Table XI

Difluorobromomethane

C-Br = 1.915 Kx., C-F = 1.35 Kx.,  $\angle$ FCBr = 110

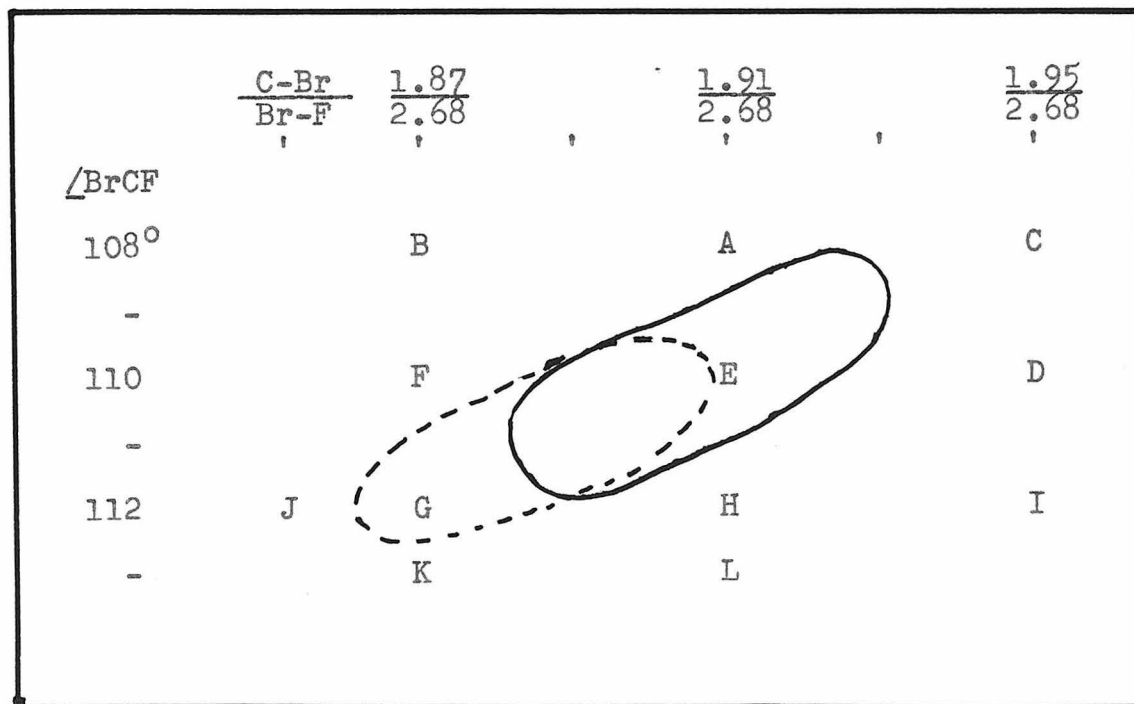
<u>Max.</u>	<u>Min.</u>	<u>q<sub>o</sub></u>	<u>q<sub>c</sub></u>	<u><math>\frac{q_c}{q_o}</math></u>
1		--	--	--
	1	( 6.83)	( 6.35)	(0.9297)
2		(10.28)	( 9.80)	(0.9533)
	2	(13.59)	(13.25)	(0.9749)
3		(17.14)	(16.80)	(0.9801)
	3	20.26	20.35	1.0044
4		24.31	24.10	0.9913
	4	27.96	27.95	0.9996
5		32.11	32.15	1.0012
	5	35.62	36.00	1.0106
6		38.81	39.00	1.0048
	6	42.78	42.50	0.9934
7		46.40	46.50	1.0021
	7	50.20	50.50	1.0059
8		54.29	54.25	0.9992
	8	58.36	58.20	0.9972
9		62.35	62.18	0.9973
	9	65.39	65.45	1.0009
10		68.70	68.25	0.9934
	10	72.50	72.20	0.9959
11		76.10	76.20	1.0013
	11	80.10	80.30	1.0025
12		84.00	84.15	1.0018
	12	87.70	87.80	1.0011
13		92.00	91.50	0.9946
	13	94.90	95.20	1.0032
14		98.40	98.65	1.0025

Average 1.0002

Average deviation 0.35%

TRIFLUOROBROMOMETHANE. The radial distribution integral, R (Fig. 18), calculated from the visual interpretation, V (Fig. 18), indicates bonded distances of 1.35 Kx. (C-F) and 1.90 Kx. (C-Br), and unbonded distances of 2.20 Kx. (F...F) and 2.68 Kx. (F...Br), giving calculated bond angles of FCF 109° and FCB 110°. Theoretical intensity curves (Figs. 17 & 18) were calculated under the assumption of C<sub>3v</sub> symmetry and with a systematic variation of the shape of the model around the radial distribution value. The shape parameters were the  $\frac{\text{Br-F}}{\text{C-Br}}$  ratio and the FCB angle. The Br-F distance was taken as 2.68 Kx. for all models.

Figure 17



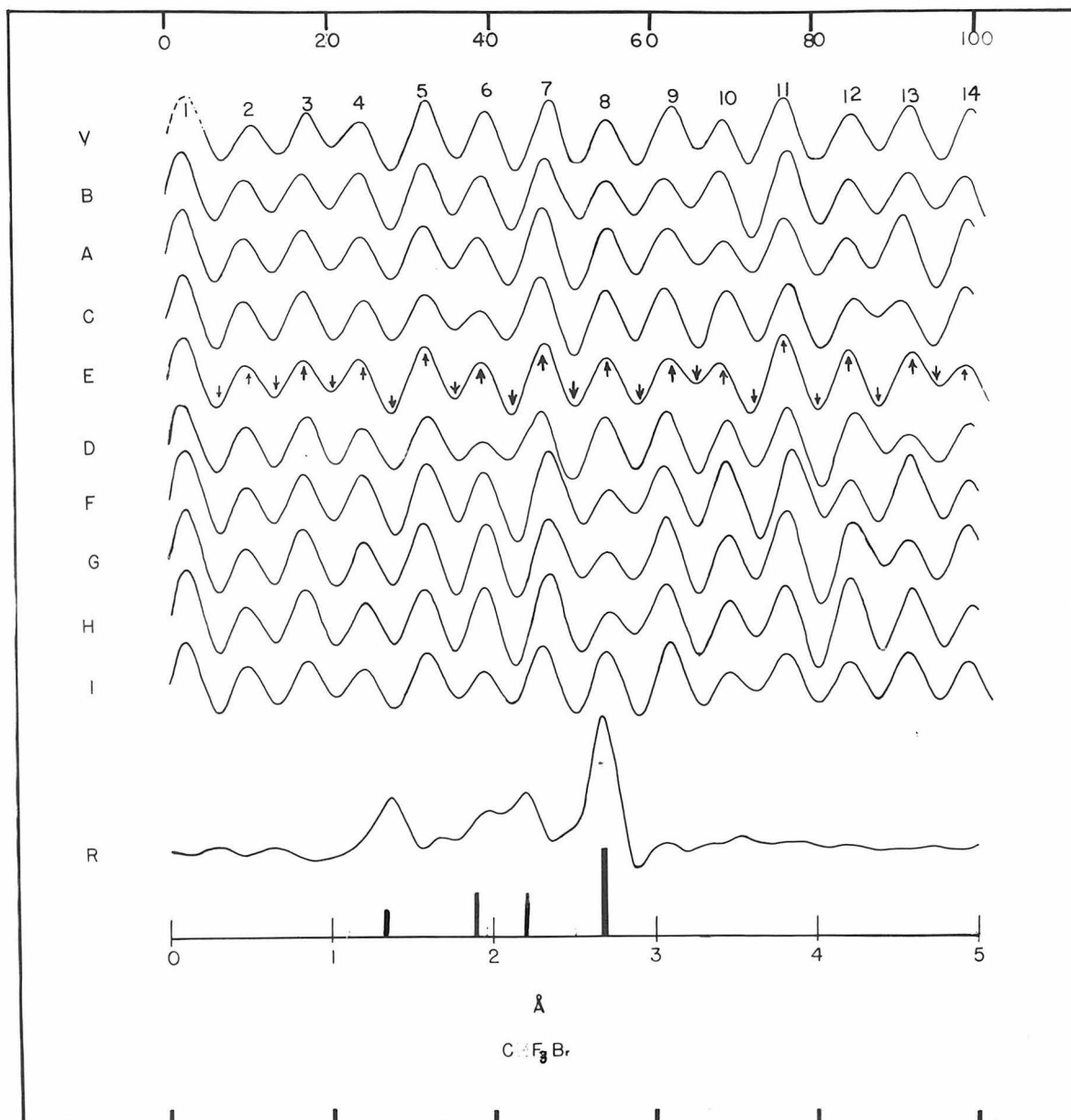


Figure 18

Trifluorobromomethane

Table XIITrifluorobromomethaneC-Br = 1.90 Kx., C-F = 1.35 Kx.,  $\angle$ FCBr = 110°

<u>Max.</u>	<u>Min.</u>	<u>q<sub>o</sub></u>	<u>q<sub>c</sub></u>	<u><math>\frac{q_c}{q_o}</math></u>
1		--	--	--
	1	( 6.7)	( 6.3)	--
2		(10.7)	( 9.9)	--
	2	(14.11)	(13.3)	--
3		17.13	17.20	1.0041
	3	20.77	20.70	0.9966
4		24.27	24.00	0.9889
	4	27.90	27.80	0.9964
5		32.00	31.85	0.9953
	5	36.02	35.65	0.9897
6		39.67	39.30	0.9907
	6	43.33	42.90	0.9901
7		47.13	47.00	0.9972
	7	50.83	50.70	0.9974
8		54.30	54.50	1.0037
	8	57.98	58.25	1.0047
9		62.17	62.20	1.0005
	9	65.40	65.60	1.0031
10		68.62	68.70	1.0012
	10	71.70	72.30	1.0084
11		75.70	76.50	1.0106
	11	80.06	80.50	1.0055
12		84.00	84.15	1.0018
	12	87.78	88.00	1.0025
13		91.56	91.95	1.0042
	13	95.63	95.80	1.0018
14		99.32	98.75	0.9943
	14	102.11	102.55	1.0043
15		105.70	106.50	1.0076

Average 1.0000  
Average deviation 0.50%

Dr. Schomaker more recently has made a visual interpretation (not shown) of the photographs. The dotted ellipse shows the range of acceptability for Dr. Schomaker's visual interpretation, the solid ellipse shows the range of acceptability for V (Fig. 18). The results on the basis of the visual observations of the author are C-Br  $1.90 \pm 0.03$  Kx., C-F  $1.35 \pm 0.03$  Kx., Br-F  $2.68 \pm 0.02$  Kx., and FCBr angle  $110 \pm 2^\circ$ . The results based on Dr. Schomaker's visual interpretation are C-Br  $1.88 \pm 0.03$  Kx., C-F  $1.35 \pm 0.03$  Kx., F-Br  $2.68 \pm 0.02$  Kx., and FCBr angle  $111 \pm 1.5^\circ$ . The final results are C-Br  $1.89 \pm 0.03$  Kx., C-F  $1.35 \pm 0.03$  Kx., Br-F  $2.68 \pm 0.02$  Kx., and BrCF angle  $110.5 \pm 2^\circ$ . Table XII shows the agreement between observed and calculated  $\underline{q}$  values for the author's final model. Table XIII shows the agreement of calculated (final model) and observed  $\underline{q}$  values for the visual interpretation of Dr. Schomaker.

TRICHLOROBROMOMETHANE. The radial distribution integral, R (Fig. 20), calculated from the visual interpretation, V (Fig. 20), indicates bonded distances of 1.85 Kx. (average C-Cl and C-Br) and unbonded distances of 2.94 Kx. (average Cl-Cl and Cl-Br). The molecule has  $C_{3v}$  symmetry (38). Theoretical intensity curves (Figs. 19 & 20) were calculated by changing the ratio  $\frac{Cl-C}{C-Br}$  and the ClCBr angle. The C-Cl distance was taken as 1.76 Kx. for all models.

Table XIII

Trifluorobromomethane

C-Br = 1.88 Kx., C-F = 1.35 Kx.,  $\angle$ FCBr = 111°

<u>Max.</u>	<u>Min.</u>	<u>q<sub>o</sub></u>	<u>q<sub>c</sub></u>	<u><math>\frac{q_c}{q_o}</math></u>
1		--	--	--
	1	( 6.7)	( 6.3)	(0.9403)
2		(10.7)	( 9.85)	(0.9207)
	2	(14.11)	(13.3)	(0.9426)
3		17.13	17.07	0.9965
	3	20.77	20.60	0.9917
4		24.27	24.15	0.9951
	4	27.90	27.85	0.9982
5		32.00	31.93	0.9978
	5	36.02	35.65	0.9893
6		39.67	39.30	0.9907
	6	43.33	43.00	0.9929
7		47.13	47.05	0.9983
	7	50.83	51.00	1.0033
8		54.30	54.50	1.0037
	8	57.98	58.25	1.0047
9		62.17	62.00	0.9973
	9	65.40	65.40	1.0000
10		68.62	68.65	1.0004
	10	71.70	72.50	1.0111
11		75.70	76.70	1.0130
	11	80.06	80.75	1.0086
12		84.00	84.33	1.0039
	12	87.78	88.15	1.0042
13		91.56	92.00	1.0047
	13	95.63	95.58	1.0005
14		99.32	99.90	1.0059
	14	102.11	102.65	1.0053
15		105.70	106.70	1.0095

Average 1.0010

Average deviation 0.52%

Figure 19

	$\frac{\text{Cl-C}}{\text{C-Br}}$	$\frac{1.76}{1.87}$		$\frac{1.76}{1.91}$		$\frac{1.76}{1.95}$
$\angle \text{ClCBr}$						
106°		A		B		C
-						
109		D		E		F
-						
112		G		H		I

The final parameters are C-Cl  $1.76 \pm 0.03$  Kx., C-Br  $1.91 \pm 0.03$  Kx., Br-Cl  $3.00 \pm 0.03$  Kx., Cl-Cl  $2.87 \pm 0.03$  Kx., and ClCBr angle  $110 \pm 2^\circ$ . Table XIV shows the agreement between observed and calculated  $q$  values for the accepted model, E. The 2.01 Kx. C-Br distance reported by Capron and Hemptinne (39) is unacceptable.

DIFLUORODIBROMOMETHANE. The radial distribution function, R (Fig. 22), calculated from the visual interpretation, V (Fig. 22), indicates bonded distances of 1.38 Kx. (C-F) and 1.91 Kx. (C-Br), and unbonded distances of 2.23 Kx. (F-F), 2.67 Kx. (Br-F), and 3.14 Kx. (Br-Br). Theoretical models (Figs. 21 & 22) were calculated for different values of the ratio of  $\frac{\text{Br-Br}}{\text{Br-F}}$  and the  $\frac{\text{C-F}}{\text{C-Br}}$  distances; the C-F distance was assumed to be 1.36 Kx. and the Br-F distance was taken as 2.67 Kx. for all models.

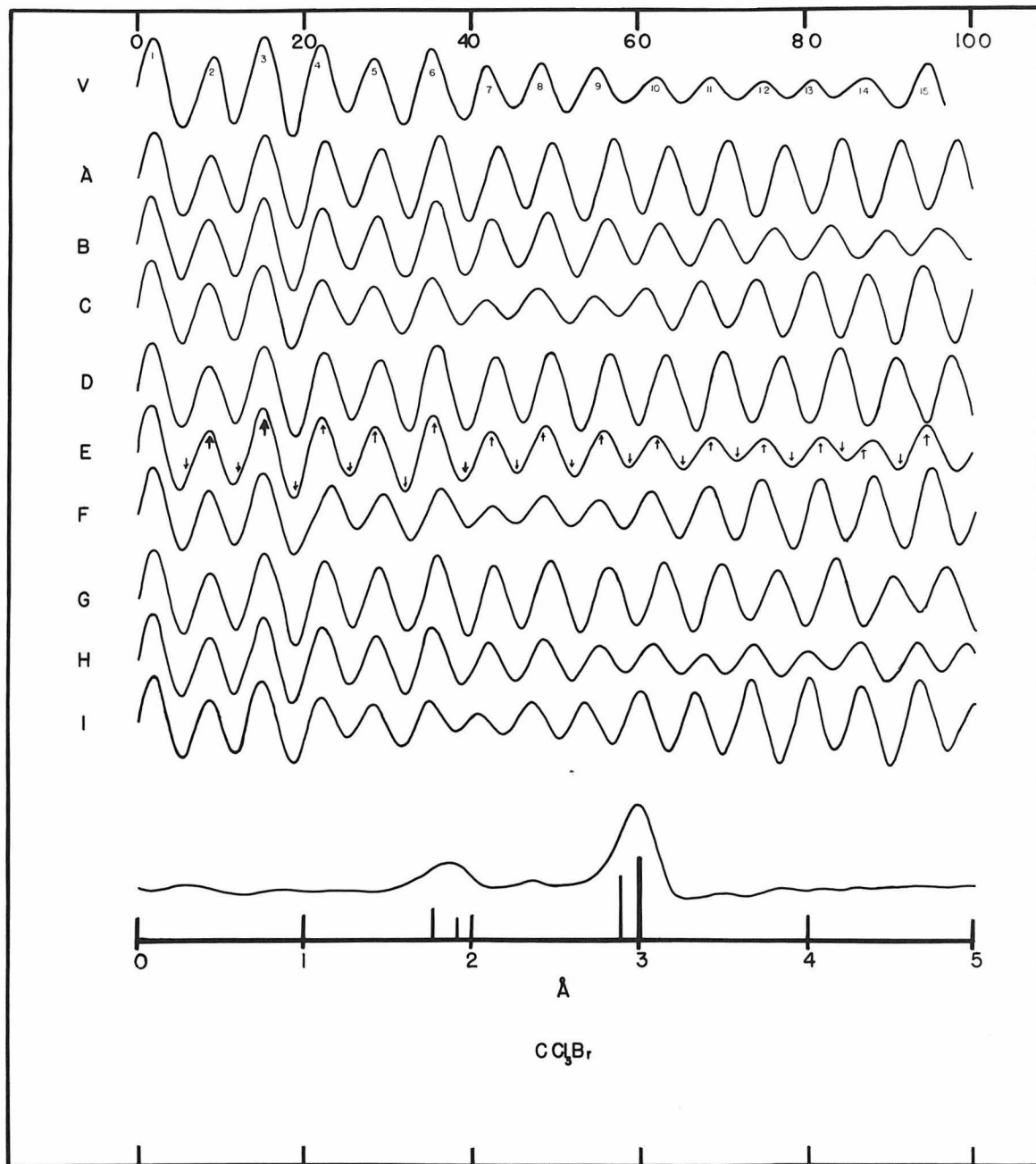


Figure 20

Trichlorobromomethane

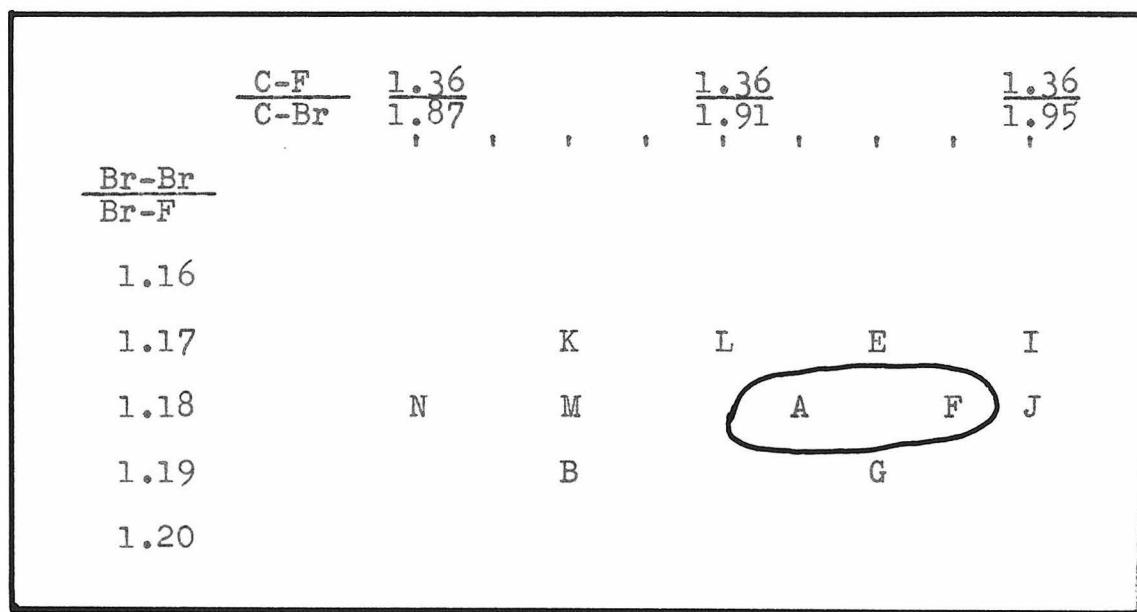
Table XIVTrichlorobromomethaneC-Cl = 1.76 Kx., C-Br = 1.91 Kx.,  $\angle\text{ClCBr} = 110^\circ$ 

<u>Max.</u>	<u>Min.</u>	<u>q<sub>o</sub></u>	<u>q<sub>c</sub></u>	<u><math>\frac{q_c}{q_o}</math></u>
1		--	--	--
	1	( 5.95)	( 5.45)	(0.9120)
2		( 8.67)	( 8.75)	(1.0116)
	2	(12.16)	(11.80)	(0.9704)
3		(15.32)	(15.15)	(0.9898)
	3	(18.88)	(18.75)	(0.9889)
4		(22.36)	(22.25)	(0.9951)
	4	25.49	25.50	1.0004
5		28.61	28.50	0.9962
	5	32.14	32.10	0.9988
6		35.61	35.50	0.9969
	6	39.30	39.50	1.0051
7		42.50	42.30	0.9953
	7	45.40	45.40	1.0000
8		48.63	48.75	1.0025
	8	51.75	52.20	1.0087
9		55.41	55.70	1.0052
	9	58.85	58.70	0.9975
10		62.32	62.20	0.9981
	10	65.29	65.30	1.0002
11		68.63	68.80	1.0025
	11	71.90	71.80	0.9986
12		75.06	75.10	1.0005
	12	78.00	78.30	1.0038
13		81.11	81.60	1.0060
	13	83.42	84.60	1.0141
14		87.33	87.70	1.0042
	14	91.36	91.20	0.9982
15		94.52	94.60	1.0008

Average 1.0015

Average deviation 0.35%

Figure 21



The best model lies between A and F. The final parameters are C-F 1.36 - (assumed), FCF angle  $109^\circ$  (calc'd.), C-Br  $1.93 \pm 0.03$  Kx., BrCF angle  $109 \pm 2^\circ$ , BrCBr angle  $110 \pm 2^\circ$ , Br-F  $2.67 \pm 0.02$  Kx., and Br-Br  $3.15 \pm 0.03$  Kx.

The limit of error, as given, on the BrCF angle is independent of the assumption of  $109^\circ$  for the FCF angle. On the basis of the  $109^\circ$  value for the FCF angle the limit of error would be  $\pm \frac{1}{2}^\circ$ . Table XV shows the agreement of calculated (average of A and F) and observed  $q$  values for the best curve.

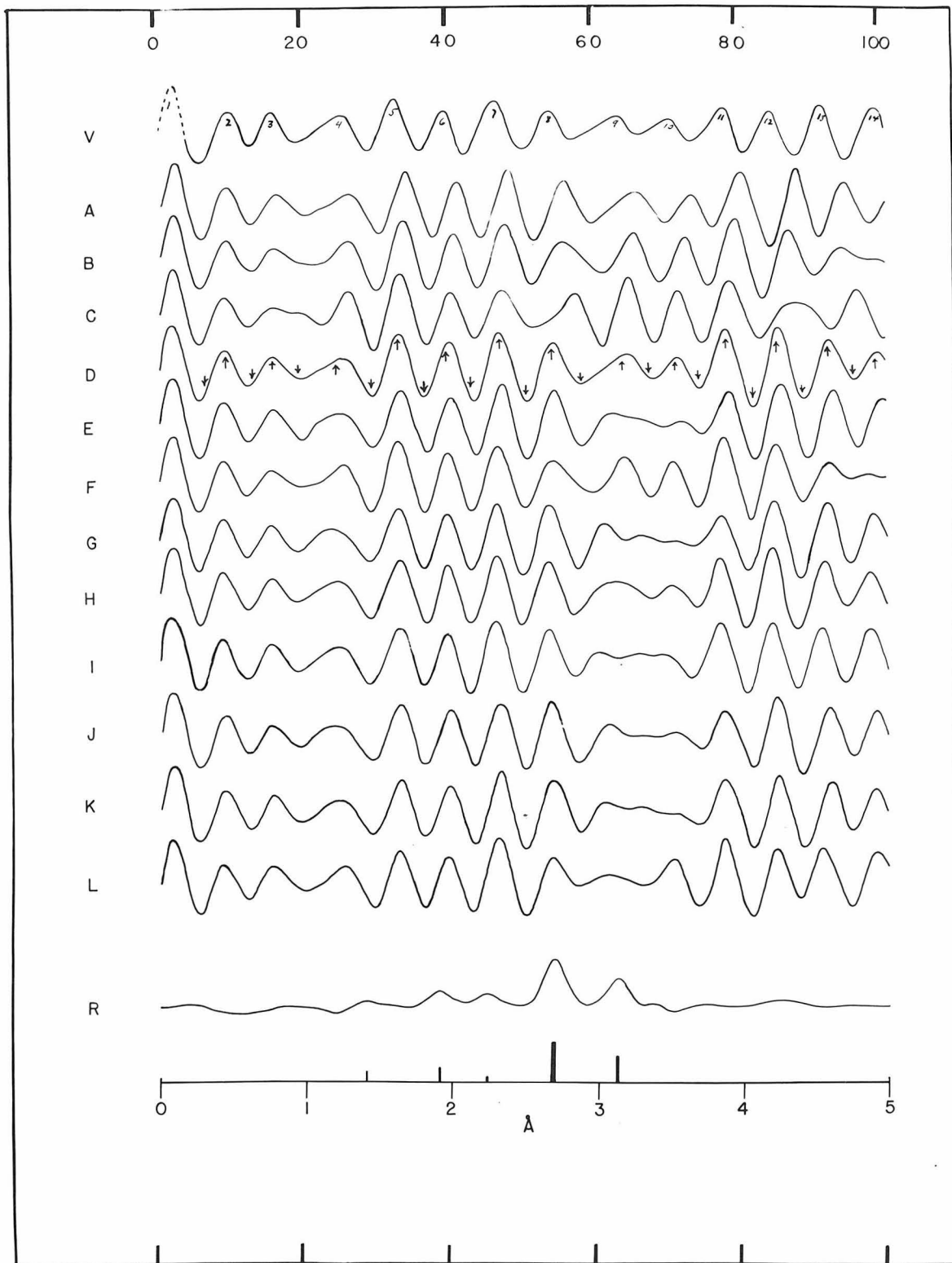


Figure 22

Difluorodibromomethane

Table XV

DifluorodibromomethaneC-F =  $1.36 \pm 0.06$  Kx., C-Br =  $1.93 \pm 0.04$  Kx.,  $\angle\text{BrCBr} = 110^\circ$ 

Max.	Min.	$q_o$	$q_c$	$\frac{q_c}{q_o}$
1		--	--	--
	1	( 5.4)	( 6.2)	(0.8710)
2		( 9.0)	( 9.0)	(1.0000)
	2	(12.1)	(12.6)	(0.9603)
3		(15.4)	(15.51)	(0.9910)
	3	(19.3)	(18.98)	(1.0163)
4		(24.9)	(23.92)	(1.0169)
	4	28.90	28.89	1.0000
5		32.60	32.56	1.0003
	5	36.1	36.38	0.9920
6		39.50	39.19	1.0074
	6	42.75	42.57	1.0038
7		46.20	46.53	0.9933
	7	50.00	50.16	0.9970
8		53.55	53.72	0.9968
	8	(56.90)	(57.78)	(0.9842)
9		63.55	63.54	1.0000
	9	66.75	66.48	1.0038
10		70.55	70.96	0.9945
	10	73.40	74.00	0.9919
11		76.95	77.72	0.9900
	11	80.55	80.76	0.9975
12		84.25	83.91	1.0041
	12	87.60	87.09	1.0057
13		91.10	90.83	1.0028
	13	94.45	94.84	0.9958
14		97.75	97.55	1.0018

Average 0.9989

Average deviation 0.45%

DISCUSSION. The dibrominated methyl fluorides tend to release bromine even when sealed in glass (40). This is in accord with the longer C-Br distance, 1.93 Kx., found for dibromodifluoromethane than is found in most brominated hydrocarbons, 1.91 Kx. Trifluorobromomethane is more stable than most hydrocarbon bromides (40), and the C-Br distance found was 1.89 Kx., a 0.02 Kx. shortening from the normal value. No significant deviation in the C-F distances was found in these compounds.

RESULTS\*

Trifluorobromomethane

$$\begin{aligned} \text{C-F} &= 1.35 \pm 0.03 \text{ Kx.} \\ \text{C-Br} &= 1.89 \pm 0.03 \text{ Kx.} \\ \angle \text{FCBr} &= 110.5 \pm 2^\circ \end{aligned}$$

Dibromodifluoromethane

$$\begin{aligned} \text{C-F} &= (1.36 \text{ Kx.}) \\ \text{C-Br} &= 1.925 \pm 0.03 \text{ Kx.} \\ \angle \text{BrCBr} &= 110 \pm 2^\circ \\ \angle \text{FCBr} &= 109 \pm 2^\circ \end{aligned}$$

Difluorobromomethane

$$\begin{aligned} \text{C-F} &= 1.35 \pm 0.03 \text{ Kx.} \\ \text{C-Br} &= 1.91 \pm 0.03 \text{ Kx.} \\ \angle \text{FCBr} &= 110 \pm 2^\circ \end{aligned}$$

Trichlorobromomethane

$$\begin{aligned} \text{C-Cl} &= 1.76 \pm 0.03 \text{ Kx.} \\ \text{C-Br} &= 1.91 \pm 0.03 \text{ Kx.} \\ \angle \text{ClCBr} &= 110 \pm 2^\circ \end{aligned}$$

---

\* Values in parentheses are assumed.

Several theoretical calculations (38) of the HCH bond angle have been made. Coulson and Moffitt predict an HCH angle of  $113^\circ$  and a shortening of the C-C distance; both results are in general agreement with this investigation. The  $121^\circ$  angle calculated by Kilpatrick and Spitzer is unacceptable on the basis of our results.

The original article by Bastiansen and Hassel (33) has been made available since the rest of the thesis was written. They report the following parameters: C-C = 1.535 Kx. (in a footnote), C-H = 1.08 Kx., HCH angle  $118.2^\circ$ , and CCH angle  $116.2^\circ$ , with a reported probable error in the angle of  $2^\circ$ . It is not clear for which angle this probable error is reported; the error in the CCH angle is only one-fourth as large as the error in the HCH angle. An error of  $8^\circ$  in the HCH angle ( $2^\circ$  in the CCH angles) would make it possible to obtain agreement with the spectroscopic results.

BIBLIOGRAPHY

1. L. K. Frevel, J.A.C.S., 58, 779-782 (1936).  
S. B. Hendricks and L. Pauling, J.A.C.S., 47, 2904-2920 (1925).
2. I. E. Knaggs, Proc. Roy. Soc., A, 150, 576-602 (1935)  
E. W. Hughes, J.C.P., 3, 1-5 (1935).
3. M. Bassiere, Compt. rend., 201, 735-737 (1935).
4. C. D. West, Z. Krist., 95, 421-425 (1936).
5. E. W. Hughes, Thesis, Cornell University (1935) and later work.
6. Heinz Wilsdorf, Acta Cryst., 1, 115 (1948).
7. Verner Schomaker, unpublished work.
8. A. D. Booth, Trans. Faraday Soc., 41, 434-439 (1945).
9. E. W. Hughes, unpublished work.
10. L. K. Frevel, Z. Krist., 94, 197 (1936).
11. L. Pauling, J.A.C.S., 69, 542 (1947).
12. Heinz Wilsdorf, Acta Cryst., 1, 115 (1948).
13. P. A. Schaffer, Jr., Verner Schomaker, and Linus Pauling, J.C.P., 14, 648-658 (1946).
14. N. W. Taylor and S. S. Cole, J.A.C.S., 56, 1648 (1934).
15. L. McCulloch, J.A.C.S., 59, 2650 (1937).
16. F. C. Kracek, G. W. Morey, and H. E. Merwin, A.J. of Sci., 35a, 143 (1938).
17. G. W. Morey and H. E. Merwin, J.A.C.S., 58, 2248 (1936).
18. C. W. Jacobs and B. E. Warren, J.A.C.S., 59, 2588 (1937).
19. A. Hettich, Z. Krist., 91, 154 (1935).
20. D. P. Shoemaker, Thesis, California Institute of Technology (1947).
21. David Harker, Meeting A.S.X.R.E.D. (April 1948).
22. E. W. Hughes, unpublished work.
23. A. L. Patterson, Z. Krist., 90, 517-542 (1935).
24. Linus Pauling, Nature of the Chemical Bond, Cornell University Press (1942).
25. W. H. Zachariasen, Z. Krist., 88, 150-161 (1934).
26. G. E. R. Schulze, Z. Physik. Chem., 24, 215-240 (1934).
27. B. E. Warren, H. Krutter, and O. Morningstar, J. Am. Ceram. Soc., 19, 202-206 (1936).
28. L. R. Maxwell, J. Opt. Soc., 30, 374 (1940).  
Walter Gordy, James W. Simmons and A. G. Smith, Phys. Rev., 74, 243 (1948).
29. L. O. Brockway, Rev. Modern Phys., 8, 231 (1936).
30. C. S. Lu and E. W. Malmberg, Rev. Sci. Instr., 14, 271 (1943).
31. P. A. Schaffer, Jr., Verner Schomaker, and Linus Pauling, J.C.P., 14, 648-658 (1946).

32. L. Pauling and L. O. Brockway, J.A.C.S., 59, 1223 (1937).
33. O. Bastiansen and O. Hassel, Tids. Kjem. Bergv. Met., 6, 71-72 (1946).
34. Gerhard Herzberg, Infra-Red and Raman Spectra, D. Van Nostrand Co., Inc. (1945).
35. L. G. Smith, Phys. Rev., 59, 924 (1941).
36. P. G. Ackermann and J. E. Mayer, J. Chem. Phys., 4, 377 (1936).
37. E. H. Eyster, Thesis, California Institute of Technology, (1938).
38. C. A. Coulson and W. E. Moffitt, J. Chem. Phys., 15, 151 (1947).  
J. E. Kilpatrick and R. W. Spitzer, J. Chem. Phys. 14, 463 (1946).
39. P. Capron and M. de Hemptinne, Sci. Abst., 40, 207 (1937).
40. J. J. Brice, W. H. Pearlson, and J. H. Simons, J.A.C.S., 68, 968 (1946).

Propositions Submitted by Heinz G. Pfeiffer

Ph.D. Oral Examination, Nov. 10, 1948, 9:00 A.M., Crellin Conference Room  
Committee: Professors Schomaker (Chairman), Hughes, Corey, Bates, Yost,  
Zechmeister, Neher and Kirkwood.

1. The sum,  $\sum_h \sum_k F_{hkz} \cos(hx + ky)$  is valuable in certain cases because it eliminates atoms in certain of the special positions in some of the space groups and also gives approximate  $z$  parameters.

2. (a) In electrophoretic experiments the optimum density gradient can be obtained by working as close to the freezing point of the solution as possible.

S. Swingle, Thesis, California Institute of Technology, 1943.

(b) The quality of the results obtained by the present methods is not noticeably affected by temperature deviations as great as  $10^\circ$  from the optimum value as long as the temperature is kept constant in the course of the experiment.

3. (a) In the method outlined in this thesis for determining the scale and temperature factors simultaneously care must be exercised in choosing a suitable method of averaging  $S^2$  over the intervals covered by the normal equations.

(b) A weighing factor  $S^2 e^{-as^2}$  or  $\frac{1}{(\sum f_i)^2}$  applied to the observed  $|F\psi_s|$  would improve the results.

4. (a) A tabulation of temperature factors used in various structure determinations would be of value.

(b) A system of cataloging electron diffraction photographs for purposes of analysis is proposed.

5. The C-H distance in ethane\*, 1.11Å should be used in spectroscopic or electron diffraction investigations of substituted methanes in cases where it is necessary to assume a value of this distance to determine a structure rather than the methane value of 1.09Å.

\* L. Smith and A. Woodward J.C.P. 386, 1942.

V. Schomaker and K. Hedberg, Electron diffraction investigation of ethane now in progress at this laboratory.

6. (a) Electron diffraction methods which rely entirely on using the data in an integrated form are a step in the wrong direction.

(b) A comparison of internal and external consistence of electron diffraction measurements would be of value in estimating the merit of an investigation.

(c) Several of the electron diffraction investigations made by Dornte have been repeated and all found in serious error. The remaining compounds investigated by Dornte should be reinvestigated for the purpose of removing errors from the literature and increasing general confidence in electron diffraction investigations.

7. (a) The C-C stretching frequency for ethylene, 1623V, cyclopentane, 886; cyclopropane 118V, spiropentane, 1083V and ethane 821V provide support for the values of the C-C distances found in these compounds by electron diffraction, 1.52 Kx, 1.34 Kx, 1.515 Kx, and 1.49 Kx.

(b) From the C-C stretching frequency of 1010V it is estimated that the C-C distance is 1.52 - 1.53 Kx. A Badger's rule calculation extrapolating between Ethane and Ethylene gives 152.75 Kx.

8. (a) In many cases it is possible to determine only some of the structure parameters by electron diffraction, by coordinating these with available spectroscopic data the complete structure can often be determined.

(b) It would be logical and valuable to be guided by spectroscopic data, when available, in choosing theoretical models for electron diffraction determinations.

9. The crystalline solid reported by Taylor and Cole (J.A.C.S. 50, 1648 (1934) as  $B_2O_3$  was probably  $HBO_2$ .

10. (a) The physiologically important esters of phosphoric acid have acid strengths greater than that of phosphoric acid itself, it is proposed that this is due to the formation of hydrogen bonds stabilizing the ion.

(b) On account of their great biochemical importance the structure of some of these esters should be determined.

11. The correlation between the meta and ortho-para directing properties of groups on disubstituted benzenes and the relative melting points of ortho, meta, and para compounds found by Holler (J. Org. Chem. 13, 70 (1948) is purely fortuitous and could be explained better on the basis of hydrogen bond formation.